A non-asymptotic sigmoid growth curve for top height growth in forest stands

Jean-Daniel Bontemps, Pierre Duplat

A non-asymptotic sigmoid growth curve for top height growth in forest stands

Jean-Daniel BONTEMPS[1,2,*], **Pierre DUPLAT**[3].

[1]AgroParisTech, ENGREF, UMR 1092 INRA/AgroParisTech Laboratoire d'Etude des Ressources Forêt-Bois (LERFoB), 14 rue Girardet, 54000 Nancy, France.

[2]INRA, Centre de Nancy, UMR 1092 INRA-AgroParisTech Laboratoire d'Etude des ressources Forêt-Bois (LERFoB), 14 rue Girardet, 54000 Nancy, France.

[3]Office National des Forêts (ONF), Département des Recherches Techniques, Boulevard de Constance, 77300, Fontainebleau, France.

* Corresponding author: jdbontemps.agroparistech@gmail.com

Summary

Since the height horizon remains undetected in the vast majority of height series sampled in forest stands, even of notable ages, the realism of the traditional asymptotic-size modelling assumption is questioned. The aim of the study was to present an original non-asymptotic growth model, and to test its accuracy against asymptotic-size equations. The equation proposed is a first-order 4-parameter autonomous differential equation. The related sigmoid size curve has a parabolic branch of time. It was tested on 349 old growth series of top height (1047 stem analyses) selected to explore the maximum observed ranges of age and site conditions, in 7 temperate tree species growing in pure and even-aged stands The fitting accuracy of this equation and three classical asymptotic-size growth equations (Richards, Hossfeld-IV, and Korf equations) were compared, with parameterisations of increasing flexibility. For the different parameterisations, the proposed growth equation showed higher performances than asymptotic growth equations, attributed to its non-asymptotic property and to the mathematical independence between parameters related to the inflection point and late growth. Top height growth was therefore accurately modelled by a sigmoid curve not based on the asymptotic-size assumption. This equation may be of general relevance to tree growth modelling.

Key words: tree height, ontogeny, late growth, top height, asymptotic size, growth equation, modelling, stem analysis, evergreen species, broadleaved species.

INTRODUCTION

Growth equations that generate sigmoid curves with asymptotic size are popular models for the description of growth (Richards, 1959; Fitzhugh, 1976). They remain a field of regular innovations (Leary *et al.*, 1997; Birch, 1999; West *et al.*, 2001; Tsoularis and Wallace, 2002; Zeide, 2004; Garcia, 2005). In long-lived species such as trees, however, the asymptotic horizon of size is not manifest in most observation data, and the biological realism of maximum tree size is being questioned (Thomas, 2002).

In radial growth, there is empirical evidence that increment – not size – may have a non-zero asymptote after a decline in the medium ontogenetic phase (Abrams *et al.*, 1999; Poage and Tappeiner, 2002; Lebourgeois *et al.*, 2004). Growth slowing is usually more salient in primary than in secondary growth, and several studies have shown that physiological and environmental constraints limit the height of trees (Ryan and Yoder, 1997; Karlsson, 2000; Koch *et al.*, 2004). However, upper limits to tree height also remain undetected in growth trajectories observed in forest stands, where trees experience competition, even at ages over 200 years (Smith, 1984; Pretzsch, 1996; Duplat and Tran-Ha, 1997, Bontemps *et al.*, 2009). Early asymptotic patterns of tree height have been detected only in the particular conditions of open-grown trees (Minckler, 1955; Ek, 1971; Mäkelä and Sievänen, 1992; Uhl *et al.*, 2006). In addition, theoretical (West *et al.*, 2001) and experimental (Koch *et al.*, 2004, Woodward, 2004) investigations have provided estimates for upper limits on tree height over a hundred metres. This order of magnitude suggests that inferences on late tree growth based on standard growth series observed in managed forests are merely speculative, in a context where harvesting operations hamper the observation of late-growth phases.

When growth series are fragmental, asymptotic-size estimates obtained from statistical fits of asymptotic growth equations are strongly sensitive to the growth equation selected (Bontemps *et al.*, 2009). They can also exhibit unrealistic values (Bailey and Clutter, 1974; Shifley and Brand, 1984; Bontemps *et al.*, 2010). This has led some authors to deny biological interpretation to asymptotic size estimates obtained in such contexts (Knight, 1968) or, as an admission of weakness, to set the asymptotic size parameter constant in the related statistical fitting procedures (Shifley and Brand, 1984). While it remains theoretically plausible, the mathematical assumption of an asymptotic limit to the height of trees growing in forest stands can hardly be tested by observation, and it leads to estimates of weak biological significance. It is therefore relevant to question the prevalence of asymptotic growth equations in height growth modelling.

Although this issue has been briefly mentioned in Bredenkamp and Gregoire (1988) and Cieszewski, (2003), it has received very little attention in the forestry literature. Specific developments on growth curves based on alternative assumptions to describe late height growth remain anecdotal. Duplat and Tran-Ha (1997) proposed a sigmoid growth curve with an upper oblique asymptote (asymptotic growth rate with non-zero value), which has been successfully applied to top height growth in many

contexts (Vanniere, 1984; Claessens *et al.*, 1999). The equation however has seven parameters, which makes their interpretation difficult (Richards, 1959; Fitzhugh, 1976). Because trees experience increasing physiological constraints with size and height (Ryan and Yoder, 1997), the assumption of asymptotic stationary growth rate may also appear extreme. Since long-term increases in height growth have been reported in European forests (Elfving and Tegnhammar, 1996; Kiviste, 1999; Bontemps *et al.*, 2009), apparent stationary late growth may actually reflect these changes (Duplat and Tran-Ha, 1997).

Asymptotic size and asymptotic growth rate may be viewed as extreme assumptions for the description of tree height growth. Surprisingly, intermediate assumptions have been poorly explored in growth equations. In the literature, we found one example of a sigmoid growth curve where height is assumed to asymptotically behave as a concave power function of time (Cieszewski, 2003). Though the power 1/3 postulated in this study may seem awkward, the accuracy of this equation has been highlighted. Because parabolic growth curves rely on the assumption of a continuous decline of growth over ontogeny but do not postulate any asymptotic size, they may define a sound alternative for the description of height growth patterns.

We here propose an alternative growth equation defining a sigmoid growth curve with a horizontal parabolic branch with respect to time. The equation is formulated as a 4-parameter first-order autonomous differential equation. Its accuracy was tested on top height data from seven temperate species growing in 349 pure and even-aged stands in 11 regions in France. Emphasis was placed on selecting growth data from stands of advanced ages, in various site conditions. The goodness-of-fit of this model was also compared with that of popular asymptotic-size sigmoid growth equations, namely, the Richards, the Hossfeld IV and the Korf equations (Zeide, 1993).

MATERIALS AND METHODS

Growth equations

Sigmoid growth curve with a horizontal parabolic branch

The proposed equation is a four-parameter generalisation of the fractional function tested in Bontemps *et al.* (2010). It is hereafter denoted by SPB (sigmoid with parabolic branch). It is formulated as a first order autonomous differential equation of time:

$$dh/dt = \mathrm{r}\, h^{\,\mathrm{a}} / (h + \mathrm{c})^{\,\mathrm{b}} \qquad (1)$$

with $0 < \mathrm{a} < \mathrm{b}$, where h is height, t is time, r is the vertical scale parameter or intrinsic growth rate, c is the horizontal location parameter, and a and b are shape parameters.

The growth rate in Eq. 1 admits a unique maximum R at size K_R, given by:

$$K_R = a\ c\ /\ (b - a), \qquad R = r\ a^a\ /\ b^b\ ((b - a)/c)^{(b-a)} \qquad (2)$$

Hence, the corresponding curve is sigmoid. Since a < b, the growth rate tends towards zero when *h* is large, but there is no finite value of *h* that cancels Eq. 1 (in which case *h* would define the asymptotic size). In the phase plane {*h*, *dh*/*dt*}, the graph of Eq. 1 has a vertical half tangent in *h* = 0 if a–1<0, and a horizontal one if a–1>0.

The point of inflection appears as a tangible reference point in empirical growth trajectories where the asymptote is not captured (Zeide, 2004). The equation was therefore parameterised with respect to that point. We considered the size at which the inflection point is observed as the horizontal location parameter, and the corresponding growth rate – by definition, the maximal growth rate – as the vertical scale parameter (Eq. 2). The shape parameters were rewritten with b = m2 and a = m1 m2 to ensure a lower structural correlation between them and to ease the statistical fitting procedure:

$$dh/dt = R\ (h/K_R)^{m1\ m2}\ /\ (1 - m1 + m1\ (h/K_R)^{m2}) \qquad (3)$$

with m1 < 1 and 0 < m1, m2.

A graph representing Eq. 3 in the phase plane is given in **Figure 1a**. The associated growth trajectories are illustrated in Figure 1b.

Eq. 3 has no analytical closed-form solution for *h*(*t*). A closed-form limit solution to Eq.3 (see **Supplementary Appendix 1**) is given by:

$$h(t) \sim (R\ \lambda\ K_R^{\lambda - 1}\ /\ m1)^{1/\lambda}\ t^{1/\lambda} \quad \text{when} \quad t >> 1 \qquad (4)$$

where:

$$\lambda = 1 + m2\ (1 - m1) \qquad (5)$$

Owing to the numerical restrictions on m1 and m2 (Eq. 3), we have $\lambda > 1$. Therefore, height asymptotically behaves as a concave power function of time, and the associated curve exhibits a horizontal parabolic branch (**Figure 1b**, limit trajectory illustrated in **Supplementary Appendix Figure 1**). The power $1/\lambda$ – the limit allometric scaling coefficient of height with time – is not mathematically related to K_R (Eq. 5), which implies that the curvature of the late trajectory is not structurally depending on the height of the inflection point. Also, size trajectories are asymptotically proportional to a power $1/\lambda$ of the maximal growth rate R (Eq. 4). This feature is desirable when R is assumed to reflect the effects of permanent environmental conditions on growth (the order relationship in the growth rate is conserved across sites; Garcia, 2006). The variety of trajectories generated by the SPB equation and role of the different parameters are illustrated in **Figure 2**.

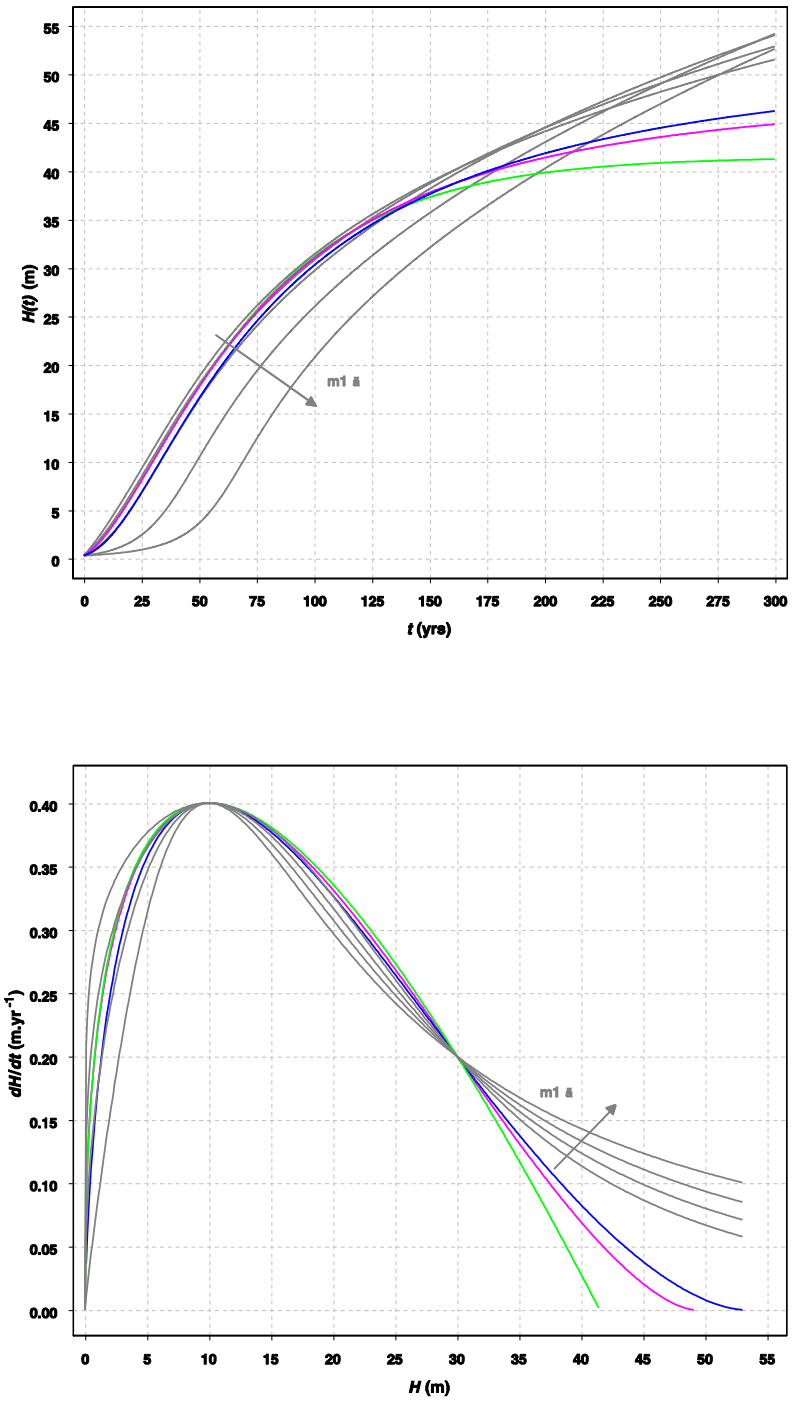

Fig. 1. Graphs of (a) the SPB and asymptotic growth equations in the phase plane and (b) the associated growth trajectories over time. To illustrate differences in late growth behaviour, equations are all represented with common constraints on early and mature growth: K_R = 10 m, R = 0.4 m.yr^{-1}, and dh/dt = 0.2 m.yr^{-1} for h = 30 m. Green: Richards equation; pink: Hossfeld equation; blue: Korf equation; grey: SPB equation, family of curves with m1 = {0.05, 0.1, 0.2, 0.4}, corresponding to m2 = {3.042, 2.613, 2.306, 2.263}. In figure 1b, an additional SPB trajectory (m1 = 0.5 and m2 = 2.397) has been plotted to better illustrate the flexibility allowed for the age of inflection point.

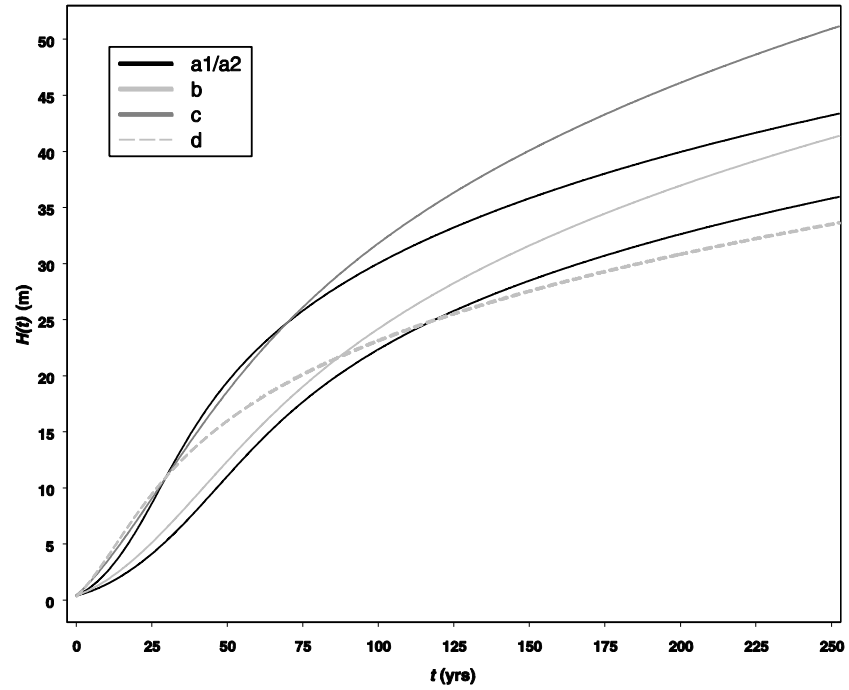

Fig. 2. Illustration of allowed variations in the shape of the SPB growth trajectory and role of the different parameters. The SPB growth trajectory is illustrated for 5 example parameterizations. To illustrate the specific role of each parameter, changes between successive parameterizations are progressive. **Parameterizations: a1/a2:** K_R = 10 m, m1 = 0.15, m2 = 3.2, R = 0.3 (lower) or 0.5 (upper) m.yr^{-1}, **b:** K_R = 10 m, m1 = 0.15, m2 = 2.6, R = 0.3 m.yr^{-1}, **c:** K_R = 10 m, m1 = 0.08, m2 = 2.6, R = 0.4 m.yr^{-1}, **d:** K_R = 5 m, m1 = 0.08, m2 = 2.6 and R = 0.4 m.yr^{-1}. Parameterizations a1 and a2 illustrate the limit anamorphic property of SPB trajectories (Eq. 4). Parameterizations b and c show the control of m2 and m1 on the parabolic branch curvature. Parameterization d reduces the sigmoid pattern by decreasing the height of inflection point.

Because the proposed equation has no analytical solution for $h(t)$, the statistical fitting procedure required a numerical integration (see Statistical Method).

Asymptotic sigmoid growth curves

The Richards, Hossfeld IV and Korf asymptotic-size sigmoid growth curves are classical equations used for growth analysis (Zeide, 1993), and were considered for comparison to the SPB growth curve. These equations contain three parameters with one shape parameter (m). They also encompass a diverse range of less-general growth equations for particular values of m: Richards is a generalisation of the Bertalanffy equation for m = 1/3 (Richards, 1959; Pienaar and Turnbull, 1973). It also includes the Mitscherlich equation for m = 1. The Hossfeld IV equation (Woollons *et al.*, 1990) includes the

logistic equation for m $\rightarrow$ 0. The Korf equation (Lundqvist, 1957) includes the Johnson-Schumacher equation for m = 1 and the Gompertz equation for m $\rightarrow$ 0.

These equations were also parameterised to replace the intrinsic growth rate by the maximal growth rate R. The asymptote K is the horizontal scale parameter of their differential forms. Expressions for the corresponding differential equations and for the height of the inflection point (K_R) are given in the **Supplementary Appendix 2**, Equations A.3 to A.5. The expression of K_R is given by:

$$K_R = K\, g(m) \qquad (6)$$

where *g* is a function of parameter m. Therefore, the asymptote K and the height of the inflection point K_R are mathematically related, and will exhibit structural correlation if m is considered global to a set of growth curves fitted and one of these parameters vary.

The graphs of these equations in the phase plane are superimposed onto that of the SPB equation in **Figure 1a**. They all have a vertical half tangent in $h = 0$. The Korf and Hossfeld equations also have a horizontal half tangent in $h = K$, while the curve of the Richards equation intersects the *h*-axis (tangent of slope $-R\ m\ C_m / K$). The convergence of the Richards curve towards its asymptote is therefore faster than that of the other asymptotic equations. The log-decline term in the Korf equation (Eq. A.5) suggests a particularly slow convergence towards the asymptote. The corresponding height trajectories are plotted in **Figure 1b**. The non-asymptotic behaviour of the SPB trajectory, as compared to asymptotic trajectories, is clearly identified over late growth.

The three equations have analytical solutions $h(t)$ (**Supplementary Appendix 2**, Eqs. A.6 to A.8). To further illustrate and compare their behaviour over late growth, equivalents for $h(t)$ when $h \rightarrow K$ ($t >> 1$) were derived based on the fundamental equivalents (Eqs. A.9 and A.10). Whereas the integrated form of the Richards equation shows exponential convergence of time, the Hossfeld and Korf equations exhibit power convergence. This may explain why the latter equations have often been found accurate for fitting tree height growth data (Woollons *et al.*, 1990; Zeide, 1993).

Growth data

We tested the generality of the proposed equation with respect to species, age range, and site fertility. The last two conditions are classical requirements for the development of site curves in pure and even-aged stand forestry (Duplat and Tran-Ha, 1997; Nord-Larsen *et al.*, 2009). Top height growth data were therefore collected from regional sampling designs of old stands covering the range of site fertility conditions, for several trees species (databases from the French Forest service, ENGREF, and INRA, 349 forest stands in total).

We selected two broadleaved species, sessile oak (*Quercus petraea* Liebl.) and common beech (*Fagus sylvatica* L.), and five coniferous species: silver fir (*Abies alba* Mill.), European larch (*Larix decidua*

Mill.), Corsican pine (*Pinus nigra* ssp. *laricio* var. 'Corsicana Hyl.'), Aleppo pine (*Pinus halepensis* Mill.), and Norway spruce (*Picea abies* Karst.; Franceschini *et al.*, 2010). Three species (sessile oak, common beech, and silver fir) were sampled in several regions, offering the opportunity to explore regional parameterisations of growth equations. A description of the dataset structure is provided in **Table 1**.

Species	**Area number**	**Regions**	**Number of plots**	**Age** (yrs)[1,2]	**Top Height** (m)[1,2]	**Sampling intensity** (yrs)
Common beech *Fagus sylvatica*	4	Normandy Lorraine / Vosges Franche-Comté Cévennes	97	142.0 (26.7) 88 – 231 years	31.7 (6.3) 10.9 – 42.3	9.0 (5.1)
Silver fir *Abies alba*	4	Vosges Cévennes Pays de Sault (SW) Southern Alps	81	114.7 (38.3) 65 – 205 years	27.4 (4.45) 19.8 – 37.5	6.9 (3.6)
Sessile oak *Quercus petraea*	5	Normandy Loire Valley Centre Lorraine	64	150.3 (28.4) 95 – 215 years	31.6 (4.0) 21.4 – 40.3	11.4 (4.7)
Corsican pine *Pinus nigra ssp. laricio v. corsicana Hyl.*	1	Corsica	34	172.5 (53.6) 85 – 270 years	29.5 (8.3) 15.2 – 44.6	5.0 (0.3)
European larch *Larix decidua*	1	Southern Alps	32	143.8 (45.0) 79 – 248 years	27.1 (5.4) 16.4 – 36.4	4.9 (0.5)
Aleppo pine *Pinus Halepensis*	1	Provence (SE)	22	89.4 (18.9) 56 – 130 years	15.1 (3.6) 7.0 – 23.7	7.9 (3.5)
Norway spruce *Picea abies*	1	Vosges	19	81.6 (35.7) 41 – 183 years	32.1 (5.7) 20.4 – 39.9	1.0 (0.0)
Total sample	17		349	129.3 (42.9) 41 – 270 years	28.8 (6.9) 7.0 – 44.6	6.1 (4.6)

Table 1. Overview of the top height growth dataset. [1]Standard-deviations are in parentheses. [2] Final age and top height of stands.

In pure and even-aged forest stands, top height is the mean height of dominant trees, defined as the 100 thickest trees at breast height per hectare. It reflects the height growth potential of tree species facing intra-specific competition in given site conditions. Past height growth of a tree can be reconstructed using stem analysis (Curtis, 1964) that relies on tree ring counts on discs sawn at different regular height intervals all along the tree stem. Top height growth can be reconstructed by

applying stem analysis to a sample of dominant trees in each stand and averaging these individual curves.

For unbiased sampling of the 100 thickest trees/ha in small-sized plots, the *n*–1 thickest trees were sampled in plots of *n*/100 ha (Pierrat *et al.*, 1995). Five dominant trees per stand were sampled in circular plots of 0.06 ha (Duplat and Tran-Ha 1997), and stem analyses were undertaken on the first, third and fifth tree. In total, 1047 trees were stem analysed as follows: (i) the first stem disc was sawn at a height of 0.30 m for most species (0.4 m for Corsican pine, 1.3 m for Norway spruce). Tree age was conventionally set to zero at this height; (ii) the second disc was sawn at a height of 1.30 m except for sessile oak (5.30 m); (iii) discs were then sawn at regular intervals along the stem, around 1–2 m for Aleppo pine, Corsican pine, European larch, and silver fir and around 2–3 m for common beech and sessile oak; (iv) the last measurement was the total tree height; (iv) for Norway spruce, stem analyses were conducted at an annual resolution (disks sampled between successive whorls). Individual tree height curves were averaged for each plot after annual linear interpolation. Average heights were calculated at points including at least one true individual tree height measurement over the three curves, for all species but Corsican pine and European larch (one point every five years, Forest Service protocol). The average sampling intensity amounted to one height observation every 6.1 yrs (SD 4.6 yrs) over the dataset. Top height and age ranges, and sampling intensity, are given for each species in Table 1. Height trajectories are plotted by species in **Figure 3**. The stem analysis protocol applied on the lower part of stems well allowed detecting the inflection point on height curves. However, there is necessary uncertainty in its location.

Available growth curves covered extended age ranges – up to 125 years in Norway spruce and Aleppo Pine, 200 years for common beech and silver fir, 225 years for sessile oak and European larch, and 250 years for Corsican pine. Within each species, a noticeable between-plot variation in growth rate was detected (**Figure 3**); for a given age, top height often varied by a factor of two between extreme curves (typically between 15 and 30 m at 100 years, Table 1). This variation was more restricted for sessile oak and Norway spruce. The late growth phase was identified in all species, but it was less apparent in sessile oak. Corsican pine was the only species to show asymptotic patterns in some height curves (for ages > 200 years). In all species, the final height of the tallest trees sampled never exceeded 45 m (25 m for Aleppo pine).

Statistical method

Data correspond to a set of tree species panel data, where time series of top height growth are observed over a collection of forest plots. Each growth equation was fitted separately to each species data, using non-linear mixed-effects models (Lappi and Bailey, 1988; Bontemps *et al.*, 2009) that account for variations in growth equation parameters according to organisation levels in the data. Here, the ‘plot’ level is the lowest. For three species, this level is nested within an additional ‘region’ level. In mixed-effects models, individual estimates of varying parameters are considered to be realisations

of random variables, whose means and standard deviations are estimated in the procedure. Growth equations were tested with several varying-parameter schemes – or parameterisations (see below). The variation of all parameters between the different growth series of a sample is not desirable as it leads to over-fitting, and does not help summarizing growth processes. Thus, at least one shape parameter was set common to the growth series of a same regional sample.

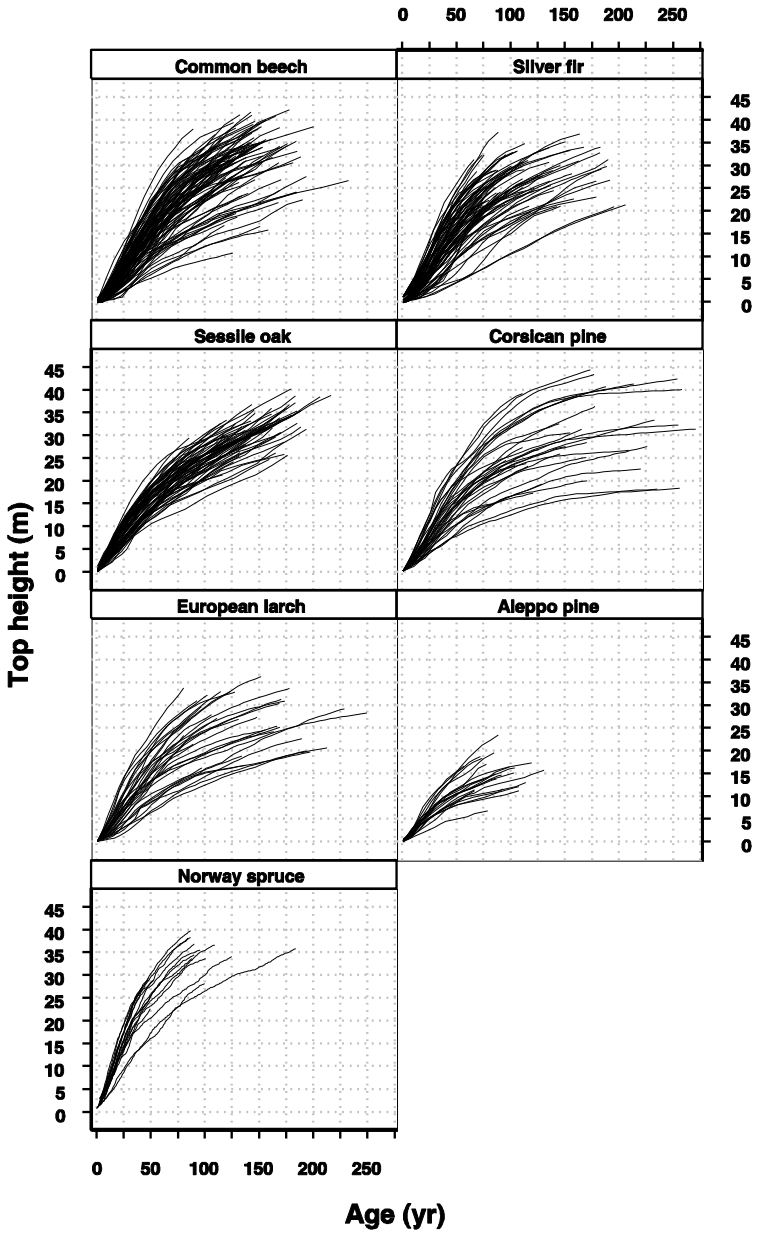

Fig. 3. Height growth trajectories of seven tree species growing in pure and even-aged forest stands. Height growth trajectories were reconstructed from 1047 stem analyses in 349 forest plots (Table 1).

Growth equations were fitted on data ordered as successive non-overlapping forward difference data: top height $h(t)$ at time t was predicted from the initial condition $h(t_{-1})$ using the integrated form of the growth equations (Eqs. A.6 to A.8, and Eq. 12 for the SPB equation), for any increment of any stand. In Norway spruce, annual increments were directly predicted from the growth differential equations (Eqs. A.3 to A.5, and Eq. 3); we identified dh/dt and h with $h(t)–h(t_{-1})$ and $h(t_{-1})$ in these equations, respectively. Models were fitted by maximum likelihood, using *nlme* procedure of the S-PLUS software. Random effects and errors were assumed to be independent with Gaussian distribution (Lindström and Bates, 1990).

Parameterisation 1. A basic parameterisation was tested in which only maximal growth rate R had a variation between plots (**Figure 3**) and other parameters remained global over each regional sample data:

$$h(t) = f\,(h(t_{-1}), \mathrm{p}) + \varepsilon[t_{-1}, t] \qquad (7)$$

$$\mathrm{p} = \{\mathrm{R}, \mathrm{K_R}, \mathrm{m1}, \mathrm{m2}\} \text{ for the SPB equation, } \mathrm{p} = \{\mathrm{R}, \mathrm{K}, \mathrm{m}\} \text{ for asymptotic equations}$$

$$\mathrm{R}_i \sim N(\mathrm{R}, \sigma_\mathrm{R}) \text{ for plot } i,\ \varepsilon[t_{-1}, t] \sim N(0, \sigma)$$

where f is the integrated form of the growth equations (Eqs. A.6 to A.8 and Eq. 12), R is the mean estimate of maximal growth rate and σ_R is its standard deviation, σ is the residual standard error (RSE), and $\varepsilon[t_{-1}, t]$ is the error term of the predicted increment over the time interval $[t_{-1}, t]$.

Parameterisation 2. A between-plot variation in a second parameter, and their correlation (ρ), were tested. One option was to target a parameter controlling late growth (**Figure 3**). In the SPB equation, we thus tested a variation in parameter m2 as the main driver of late height growth (Eq. 5), since we generally observed m1<<m2 (Table 2):

$$\mathrm{R}_i \sim N(\mathrm{R}, \sigma_\mathrm{R}),\ \mathrm{m2}_i \sim N(\mathrm{m2}, \sigma_{\mathrm{m2}}),\ \rho = \mathrm{cor}\,(\mathrm{R}, \mathrm{m2}) \qquad (8)$$

However, in contrast to the asymptotic equation case, the R-families of height curves are asymptotically proportional to each other in the SPB equation (Eq. 4, **Figure 2**), and the variation of m2 together with R may be redundant. Therefore, the between-plot variation in parameter $\mathrm{K_R}$ instead of m2 was also tested:

$$\mathrm{R}_i \sim N(\mathrm{R}, \sigma_\mathrm{R}),\ \mathrm{K_{R}}_i \sim N(\mathrm{K_R}, \sigma_{\mathrm{KR}}),\ \rho = \mathrm{cor}\,(\mathrm{R}, \mathrm{K_R}) \qquad (9)$$

In the asymptotic-size equations, parameter K was selected as the second varying parameter. Because K and $\mathrm{K_R}$ are mathematically related when the shape parameter m is kept constant (Eq. 6), the variation in parameter K comes along with an implicit variation in parameter $\mathrm{K_R}$:

$$R_i \sim N(R, \sigma_R),\ K_i \sim N(K, \sigma_K),\ \rho = \text{cor}\ (R, K) \qquad (10)$$

Parameterisation 3. For three species (common beech, silver fir, and sessile oak; **Table 1**), Additional regional variation in the shape of height curves was investigated, as it has often been reported (Farr and Harris, 1979; Duplat and Tran-Ha, 1997; Bontemps *et al.*, 2011). Starting from parameterisation 2, between-region variations in shape parameters m2 of the SPB equation, and m of the asymptotic equations, were tested:

$$\text{SPB equation: } m2_j \sim N(m2, \sigma_{m2}),\ \text{asymptotic equations: } m_j \sim N(m, \sigma_m), \text{ for region } j \qquad (11)$$

For a given equation, the successive parameterisations define nested models, and they were compared using the χ^2 likelihood ratio test (LRT). Models based on different growth equations for a given species were compared using the AIC criterion, a penalisation of log-likelihood according to the number p of model parameters (AIC = 2 (p – logL)). Lower AIC indicates a better model. The use of AIC was required in particular to evaluate the accuracy of the SPB equation relative to asymptotic equations. To not bias the comparison of growth equations accuracies, these were compared for parameterizations of a given flexibility, i.e. of a same number of random parameters.

Numerical integration of SPB equation

Numerical integration was required to fit the SPB equation to pluri-annual increment data. We used the Runge–Kutta 4 (RK4) method of numerical integration (Burden and Faires, 2001, pp. 272-282) to calculate the f_{RK4} approximation of f (Eq. 7) for each increment fitted:

$$h(t) = f_{RK4}\,(h(t_{-1}), p) + \varepsilon[t_{-1}, t] \qquad (12)$$

This approximation was incorporated into a function of arguments $h(t_{-1})$ and parameter vector p, passed to the *nlme* function of S-PLUS as the predictor of $h(t)$ (see **Supplementary Appendix 3**). Precision in numerical integration depends on the number n of subintervals of integration defined over $[t_{-1}, t]$. Because the differential growth functions vary slowly on time intervals in the range of data increments (mean time interval 6.1 years, **Figure 1b**), n is typically low. This number was estimated in practice by comparing the fits of one asymptotic equation (the Korf function) obtained from both its formal solution (Eq. A.8) and the RK4 approximation. Ten iterations proved sufficient for the two fits to remain indistinguishable. This number was increased to 25 for the sake of caution.

RESULTS

Parameterisation 1

Model characteristics and parameter estimates are shown in **Table 2**.

Species	Equation	Goodness of fit					Fixed effects				Random effects
		p_f[1]	p_r[1]	logL[2]	AIC[3]	RSE[4] m	R m/yr	K/K_R[5] m	m/m1[6]	m2	σ_R m/yr
Common beech	Richards	4	1	–1675.2	3360.4	0.657	0.31	42.1	0.642	-	0.10
	Korf	4	1	–1608.4	3226.9	0.627	0.34	57.5	0.989	-	0.11
	Hossfeld	4	1	–1642.3	3294.6	0.641	0.32	48.4	0.642	-	0.10
	SPB	5	1	–1613.5	3239.0	0.629	0.35	9.1	0.138	2.620	0.11
Silver fir	Richards	4	1	–976.25	1962.5	0.453	0.35	36.3	0.501	-	0.12
	Korf	4	1	–946.0	1902.0	0.442	0.36	43.3	0.613	-	0.12
	Hossfeld	4	1	–944.0	1898.0	0.441	0.35	40.4	0.545	-	0.12
	SPB	5	1	–911.5	1835.0	0.430	0.38	9.9	0.134	3.08	0.13
Sessile oak	Richards	4	1	–852.6	1715.2	0.615	0.35	43.6	0.984	-	0.07
	Korf	4	1	–805.15	1620.3	0.579	0.36	129.3	2.636	-	0.07
	Hossfeld	4	1	–828.75	1667.5	0.596	0.35	58.9	0.929	-	0.07
	SPB	5	1	–793.4	1598.8	0.570	0.36	4.3	0.112	1.801	0.07
Corsican pine	Richards	4	1	–418.8	847.6	0.324	0.31	42.5	0.859	-	0.13
	Korf	4	1	–328.2	666.4	0.300	0.35	60.9	1.378	-	0.15
	Hossfeld	4	1	–356.4	722.8	0.307	0.32	48.3	0.767	-	0.14
	SPB	5	1	–293.6	599.3	0.291	0.35	7.8	0.081	2.914	0.15
European larch	Richards	4	1	–258.9	527.9	0.296	0.31	36.6	0.766	-	0.13
	Korf	4	1	–217.3	444.6	0.283	0.34	61.6	1.463	-	0.15
	Hossfeld	4	1	–233.5	477.0	0.288	0.32	43.7	0.735	-	0.14
	SPB	5	1	–202.6	417.1	0.278	0.34	6.6	0.114	2.404	0.15
Aleppo pine	Richards	4	1	–184.9	379.8	0.449	0.23	23.9	0.853	-	0.09
	Korf	4	1	–169.2	348.5	0.419	0.25	42.4	1.633	-	0.10
	Hossfeld	4	1	–178.3	366.7	0.436	0.23	28.7	0.790	-	0.09
	SPB	5	1	–159.9	331.8	0.402	0.27	3.3	0.301	1.917	0.10
Norway spruce	Richards	4	1	1170.7	–2331.4	0.110	0.61	41.0	0.663	-	0.15
	Korf	4	1	1232.2	–2454.3	0.106	0.65	55.0	0.947	-	0.16
	Hossfeld	4	1	1208.1	–2406.2	0.108	0.63	47.3	0.651	-	0.15
	SPB	5	1	1236.6	–2461.3	0.106	0.65	9.4	0.104	2.837	0.16

Table 2. Goodness of fit and parameter estimates for the SPB and asymptotic growth equations tested with parameterisation 1 (between-plot variation in parameter R). SPB: sigmoid with horizontal parabolic branch equation. [1]parameter number, p_f and p_r are the number of fixed and random effects, respectively; [2]log-likelihood; [3]Akaike information criterion; [4]residual standard error; [5]K is the asymptotic height for asymptotic equations, K_R is the height of the inflection point (SPB equation); [6]shape parameter m for asymptotic equations, m1 for the SPB equation.

The SPB equation provided significantly better fits in all species (-67 to -17 points in AIC relative to the second best equation, -7 points for Norway spruce) but for common beech, for which the Korf equation was more accurate (-13 points in AIC, **Table 2**). Compared with the SPB equation, the Korf equation provided the second best series of fits, except in Silver fir (Hossfeld equation). The worst fitting accuracy was always observed with the Richards equation. Depending on the species, the RSE of increment prediction was between 0.30 and 0.65 m. For Norway spruce, the annual resolution of increments led to a much smaller RSE (0.10 m).

The estimate of the mean maximal growth rate depended very little on the equation fitted. It was around 0.30-0.36 $m.yr^{-1}$ for most species (over 0.61 $m.yr^{-1}$ for Norway spruce and around 0.25 $m.yr^{-1}$ for Aleppo pine; see **Figure 3**). For the SPB equation, standard deviations of the random plot variation of R ranged from 0.07 to 0.16 $m.yr^{-1}$. Thus, associated coefficients of variation ranged from 31% to 44% for most species, indicating a substantial variation in the maximal height growth rate between forest plots. This variation was more restricted for Norway spruce (25%) and sessile oak (19%; **Figure 3**).

In the SPB equation, estimates of parameter m1 were an order of magnitude below those of m2 (**Table 2**). The estimate for the limit scaling exponent of height with time $1/\lambda$ (Eq. 5) amounted to 0.323 on average, and varied between 0.27 (Corsican pine) and 0.43 (Aleppo pine). The height of the inflection point was below 5 m for Aleppo pine and sessile oak, and between 7 and 10 m for other species. Estimates for parameter K in the asymptotic equations exhibited very strong dependence on the equation considered, and they were in accordance with the equations' asymptotic properties (**Figure 1b**): estimates from the Richards equation were the lowest (up to 43.6 m); estimates from the Korf equation were the highest (up to 129 m), and those from the Hossfeld equation were in-between (up to 59 m).

Parameterisation 2

Model characteristics and parameter estimates are shown in **Table 3**.

In the previous parameterisation, m2 was found to be quantitatively predominant in the estimate of parameter λ that controls late-growth in the SPB curve (**Table 2**). This parameter set {R, m2} was allowed to vary between stands. The {R, K_R} set of varying parameters was also tested (see Methods). In the asymptotic equations, the {R, K} set of parameters was allowed to vary between stands.

Two-varying-parameter parameterisations very significantly improved the fitting accuracy of the SPB and asymptotic equations (**Table 3**; LRT test: $p<10^{-4}$ for all tree species and equations, not presented). Variations in the set of parameters {R, K_R} in the SPB equation proved more accurate than those in {R, m2} for all tree species, with decreases in AIC of more than 50 points for most species (23 points for sessile oak, 14 points for Norway spruce). This parameterisation was retained in the next step. These two-parameter parameterisations also led to a general decrease in RSE, ranging from 0.20 to 0.55m. The RSE remained stable for Norway spruce.

Species	Equation	Goodness of fit					Fixed effects				Random effects		
		p_f[1]	p_r[1]	logL[2]	AIC[3]	RSE[4] m	R m/yr	K/K_R[5] m	m/m1[6]	m2	σ_R m/yr	σ_K m	$\rho_{R,K/KR}$
Common beech	Richards	5	2	–1537.8	3089.6	0.564	0.33	37.7	0.563	-	0.09	6.9	0.59
	Korf	5	2	–1436.8	2887.6	0.522	0.36	49.1	0.832	-	0.10	10.7	0.47
	Hossfeld	5	2	–1493.3	3000.6	0.545	0.34	43.0	0.595	-	0.09	8.5	0.53
	SPB	6	2	–1418.7	2853.5	0.515	0.38	8.1	0.182	2.47	0.10	2.2	0.34
Silver fir	Richards	5	2	–818.3	1650.6	0.375	0.37	32.8	0.404	-	0.11	4.6	0.37
	Korf	5	2	–790.3	1594.7	0.368	0.38	37.0	0.427	-	0.12	5.3	0.38
	Hossfeld	5	2	–781.1	1576.2	0.364	0.38	36.2	0.488	-	0.12	5.2	0.37
	SPB	6	2	–749.7	1515.4	0.357	0.40	9.8	0.135	3.22	0.12	1.51	0.36
Sessile oak	Richards	5	2	–820.5	1654.9	0.557	0.35	41.7	0.955	-	0.07	6.8	–0.34
	Korf	5	2	–756.3	1526.7	0.506	0.38	91.9	2.114	-	0.08	18.5	–0.46
	Hossfeld	5	2	–788.9	1591.7	0.532	0.35	54.7	0.888	-	0.07	9.9	–0.41
	SPB	6	2	–729.5	1474.9	0.490	0.38	4.4	0.120	1.80	0.08	1.08	–0.57
Corsican pine	Richards	5	2	3.9	6.2	0.215	0.35	31.7	0.656	-	0.10	8.2	0.82
	Korf	5	2	–15.4	44.7	0.221	0.38	39.1	0.829	-	0.11	9.9	0.79
	Hossfeld	5	2	33.0	–52.0	0.211	0.36	35.8	0.632	-	0.11	9.2	0.81
	SPB	6	2	24.4	–32.9	0.213	0.36	8.7	0.043	4.06	0.11	2.2	0.78
European Larch	Richards	5	2	–122.1	258.2	0.244	0.33	32.1	0.696	-	0.12	6.7	0.61
	Korf	5	2	–68.0	150.1	0.230	0.36	49.2	1.207	-	0.13	11.6	0.44
	Hossfeld	5	2	–83.4	180.9	0.234	0.34	37.9	0.685	-	0.12	8.4	0.54
	SPB	5	2	–28.6	71.2	0.219	0.36	6.9	0.097	2.75	0.13	1.74	NS
Aleppo pine	Richards	5	2	–129.1	272.2	0.336	0.25	17.8	0.653	-	0.06	4.8	0.92
	Korf	5	2	–108.25	230.5	0.302	0.27	23.9	0.958	-	0.07	7.0	0.80
	Hossfeld	5	2	–120.15	254.3	0.321	0.26	20.6	0.866	-	0.06	5.8	0.87
	SPB	6	2	–96.7	209.4	0.284	0.30	3.4	0.228	2.25	0.08	1.1	0.67
Norway spruce	Richards	4	2	1227.1	–2442.3	0.105	0.62	38.3	0.594	-	0.15	3.2	NS
	Korf	4	2	1273.3	–2534.5	0.102	0.66	49.6	0.812	-	0.15	4.1	NS
	Hossfeld	4	2	1256.4	–2500.8	0.103	0.64	44.1	0.612	-	0.15	3.7	NS
	SPB	5	2	1281.5	–2549.0	0.101	0.6	9.7	0.090	3.08	0.15	0.9	NS

Table 3. Goodness of fit and parameter estimates for the SPB and asymptotic growth equations tested with parameterisation 2 (between-plot variation in parameter R and parameter K (asymptotic equations) or K_R (SPB)). SPB: sigmoid with parabolic branch equation. [1]parameter number, p_f and p_r are the number of fixed and random effects, respectively;; [2]log-likelihood; [3]Akaike information criterion; [4]residual standard error; [5]K is the asymptotic height for asymptotic equations, K_R is the height of the inflection point (SPB equation); [6]shape parameter m for asymptotic equations, m1 for the SPB equation.

Once again, the SPB equation generally had the best fitting accuracy, with reductions in AIC from 15 to 80 points depending on the species. The exception concerned Corsican pine (best fit with the

Hossfeld equation). In general, the Korf equation again provided the second best series of fits. The Richards equation again had the lowest fitting accuracy and was not considered in further analyses.

Standard deviations for the plot variation in the asymptotic height (asymptotic equations) typically ranged from 4 to 10 m (**Table 3**). The relative variation of the asymptote (20%) was on average lower than that of the maximal growth rate and ranged from 14% (silver fir) to 28% (Aleppo pine). In Norway spruce, it was reduced down to 8%. Standard deviations for the height of the inflection point (parameterisation 2 retained for the SPB equation) ranged from 1 to 2 m, corresponding to coefficients of variation around 25% (15% for silver fir, 9% for Norway spruce). The between-plot correlation of parameters R and K_R (SPB equation) was as follows: not significant for Norway spruce and European larch, negative for sessile oak, and positive for all other tree species (**Table 3**). In the asymptotic equations, the correlation between R and K was not significant for Norway spruce, negative for sessile oak, and positive for all other tree species. In the SPB equation, the scaling exponent $1/\lambda$ was 0.30 on average, ranging from 0.20 (Corsican pine) to 0.39 (sessile oak; see **Table 4**).

Tree species	**Scaling exponent α** $H(t) \propto t^{\alpha}$ with $\alpha = 1/\{1+(m2\ (1-m1))\}$
Common beech	0.331
Silver fir	0.264
Sessile oak	0.387
Corsican pine	0.205
European larch	0.287
Aleppo pine	0.365
Norway spruce	0.263
All species average	0.300

Table 4. Limit scaling exponent of height with time (SPB equation) for the studied species. The allometry is asymptotic (see Eq. 5). Allometric coefficient estimates were obtained with the SPB equation fits of parameterisation 2 (Table 3).

Model residuals are plotted and analysed in-depth in **Supplementary Appendix 4**. Systematic underestimation of height was found at low heights and over late growth for Richards equation, and to a lesser extent for Hossfeld equation. It was less obvious in European larch and Corsican pine. For most species, underestimation of late growth was reduced using the Korf equation. However, even this equation underestimated late growth in sessile oak. By contrast, it overestimated late growth in Corsican pine (in which asymptotic patterns were evidenced; **Figure 3**). Fits obtained with the SPB

equation revealed no apparent bias across tree heights covered for most species, including sessile oak. A noticeable exception was common beech, whose concavity of height curves the SPB equation was unable to mimic (**Figure 2**).

Parameterisation 3 (common beech, silver fir, and sessile oak)

Model characteristics and parameter estimates are shown in Table 5.

	Goodness of fit					Shape parameter		Model comparisons (p-value LRT test)	
Equation	**logL**	**p_f**	**p_r**	**AIC**	**RSE**	**m/m2[1]**	**$\sigma_{m/m2}$[1]**	**regional variation**	**Hossfeld, Korf**
Common beech									
Hossfeld	-1486.2	5	3	2988.4	0.543	0.635	0.066	**0.0002**	-
Korf	-1421.4	5	3	2858.8	0.518	1.047	0.337	**<10-4**	-
SPB	-1403.7	6	3	2825.5	0.508	2.393	0.181	**<10-4**	<10-4
Silver fir									
Hossfeld	-774.5	5	3	1565.0	0.363	0.496	0.031	**0.0003**	-
Korf	-790.0	5	3	1596.0	0.368	0.432	0.020	0.41	-
SPB	-748.8	6	3	1515.6	0.356	3.192	0.110	0.17	<10-4
Sessile oak									
Hossfeld	-788.9	5	3	1593.8	0.532	0.888	<10-4	0.99	-
Korf	-755.3	5	3	1526.7	0.506	2.120	0.064	0.15	-
SPB	-726.7	6	3	1471.3	0.488	1.782	0.091	**0.02**	<10-4

Table 5. Test of additional regional variation in one shape parameter of the SPB and asymptotic equations. The test was carried out with species sampled in several regions, see Table 1. [1]parameter m in asymptotic equations, m2 in the SPB equation, see Table 4 for legends.

Improvements in the model goodness-of-fit varied widely depending on the tree species. In common beech, the regional variation in the shape parameter was significant for all equations. In silver fir, the regional parameterisation was significant only for the Hossfeld equation ($p = 0.0003$). In sessile oak, a slight improvement was observed for the SPB equation only ($p = 0.02$). Again, the SPB equation was found to be significantly more accurate than the others (**Table 5**). Residuals of the SPB equation fits (**Supplementary Appendix Figure 3**) showed that the SPB equation remained rather inaccurate for common beech, although the goodness-of-fit with that parameterisation was higher than obtained with parameterisation 2.

Fits of individual curves

Height curves fitted with the SPB equation are illustrated and compared to data in **Figure 4** (parameterisation 2 with variation in {R, K_R}, **Table 3**). Three individual curves per species were selected, both to maximise the age range covered and to illustrate the more salient aspects of the growth curve. The descriptive accuracy of the SPB curve over age range was satisfactory. The ability to mimic late growth was independent of the timing of maximal growth (early occurrence for sessile oak and Norway spruce, late for silver fir and Aleppo pine). The adequacy of the equation was more limited for late growth of Corsican pine that exhibited a more acute slowing of growth. The curvature in the height curves of common beech was stronger than that depicted in the SPB trajectories, as evidenced in **Supplementary Appendix Figure 3**. Further comparisons between these fits and those obtained with asymptotic-size equations are illustrated in **Supplementary Appendix Figure 4**.

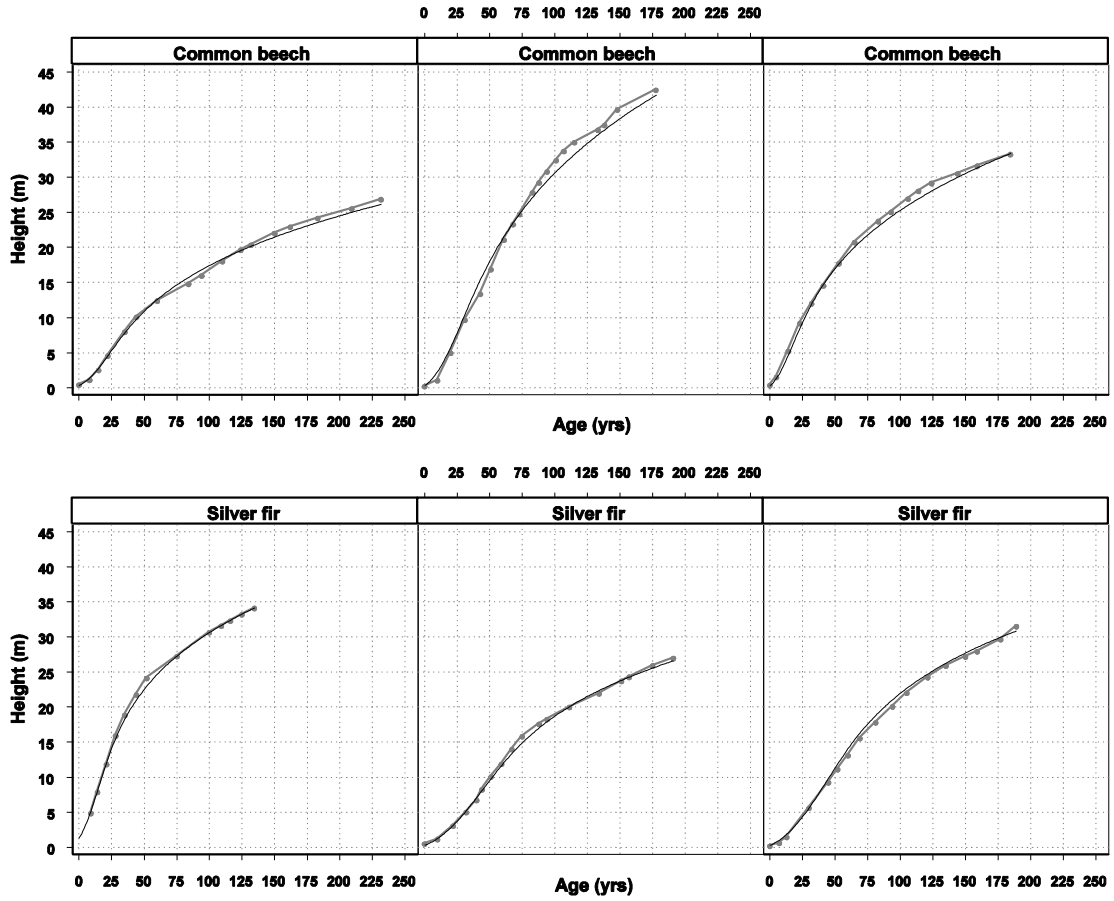

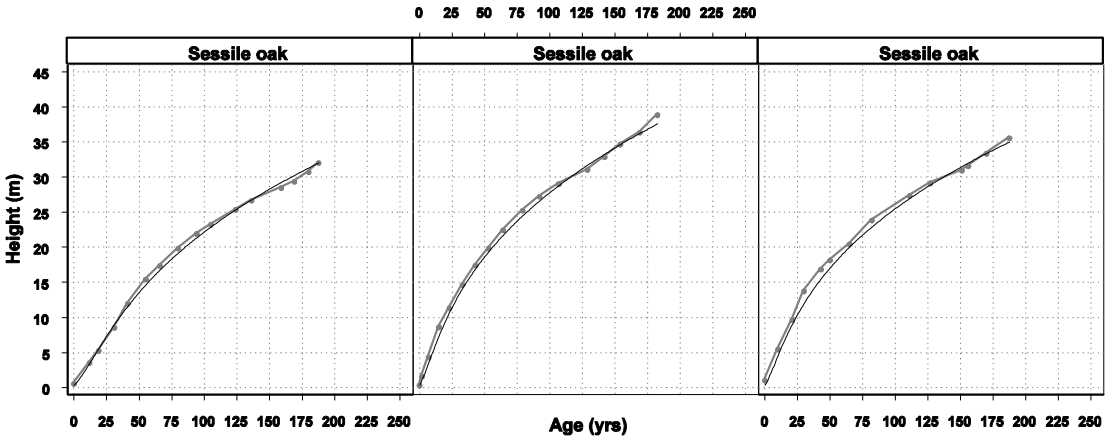
Sessile oak
Sessile oak
Sessile oak
Height (m)
Age (yrs)

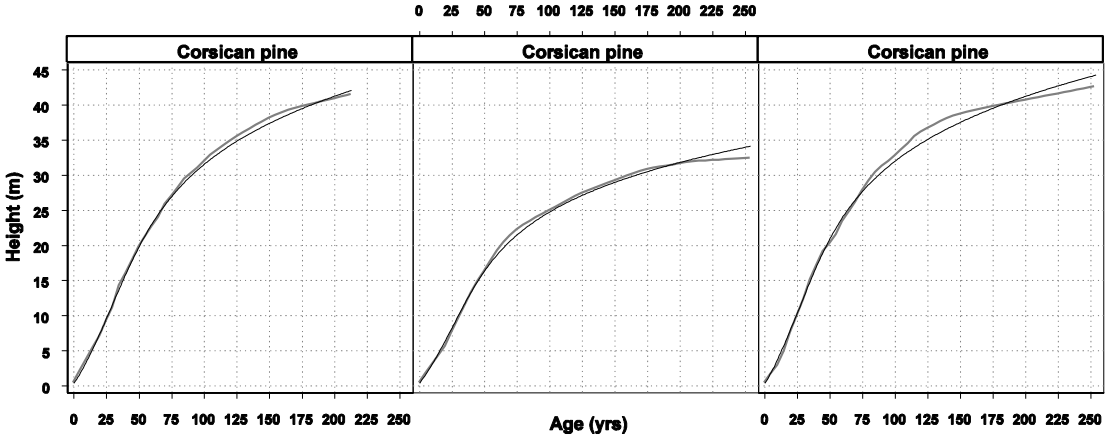
Corsican pine
Corsican pine
Corsican pine
Height (m)
Age (yrs)

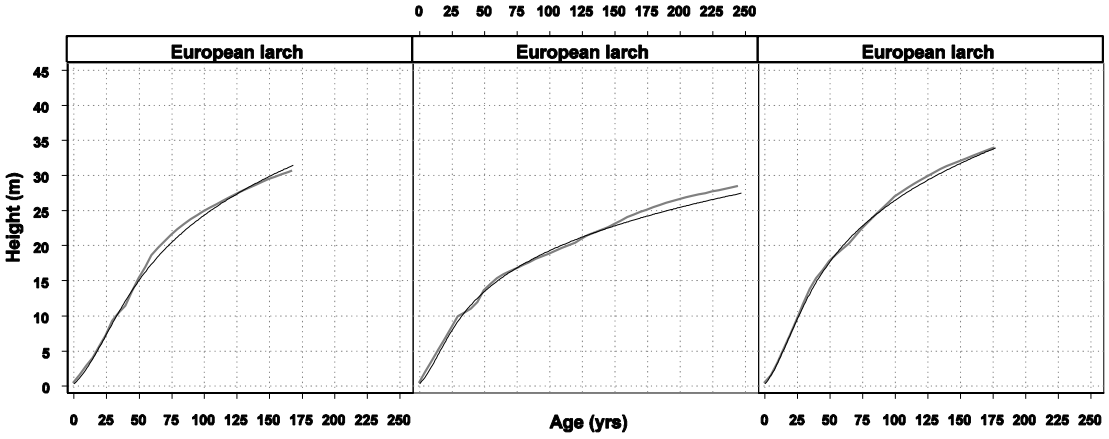
European larch
European larch
European larch
Height (m)
Age (yrs)

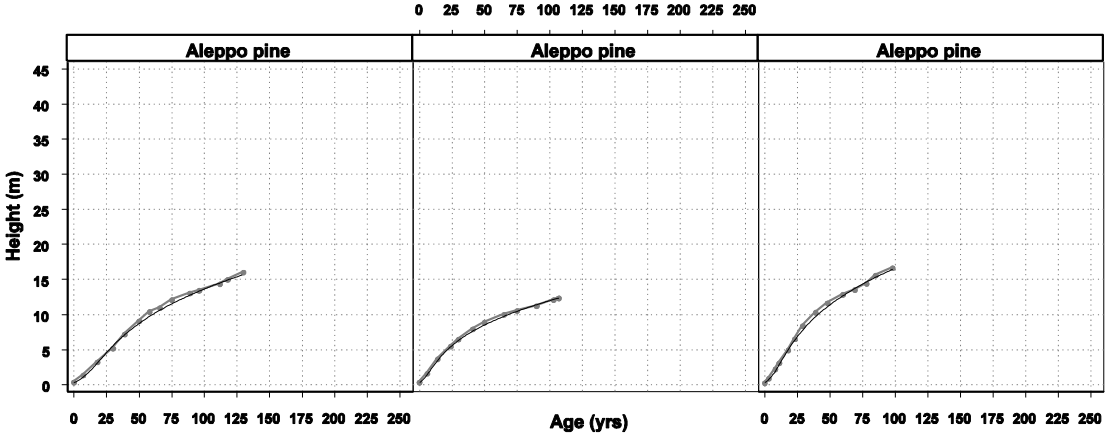
Aleppo pine
Aleppo pine
Aleppo pine
Height (m)
Age (yrs)

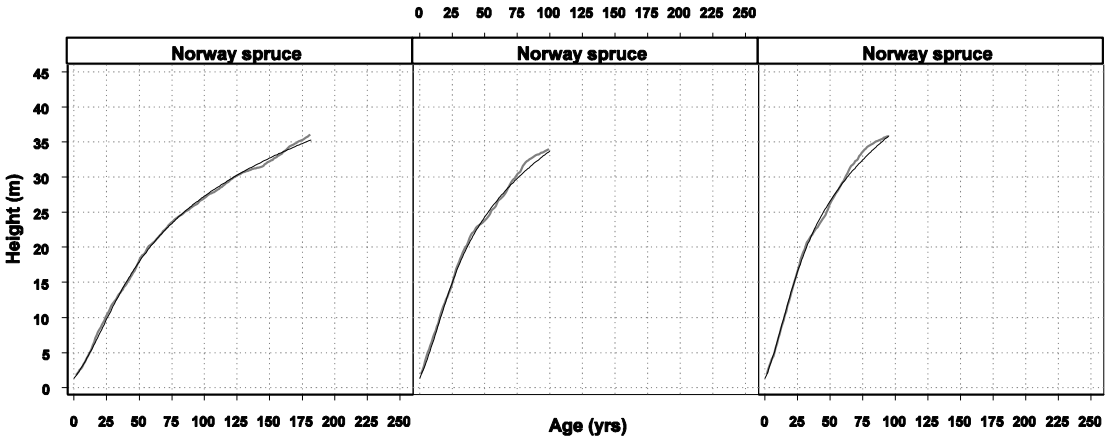

Fig. 4. Fits of height curves obtained with the SPB equation and parameterisation 2. Three plots per species were chosen to encompass the maximum age range. Thick line and dots: empirical top height curves, thin line: fitted curves.

DISCUSSION

For tree species growing in forest stands, height growth reduction over ontogeny following the early maximum is particularly slow (**Figure 3**), even when substantial age ranges are considered (**Table 1**). This makes it difficult to test the relevance of the asymptotic-size assumption, inherent to common growth equations. We tested the hypothesis that this assumption is unnecessary for a correct description of growth. We proposed a non-asymptotic sigmoid equation and tested it against asymptotic-size sigmoid equations over a top height growth dataset designed to cover broad stand age and site conditions, for a wide set of species.

Mathematical formulation of the growth equation

The equation proposed (Eqs. 1 and 3) represents growth as a fractional function of size. It is conceptually not different from the structure of asymptotic-size differential equations, in which growth is analysed as a product of expansion and decline functions of size (Leary and Holdaway, 1979; Zeide, 1993). The main difference, however, is that the decline term is an inverse function that zeroes for no finite value of size, which provides the non-asymptotic property. The point of inflection in growth rate at late growth (phase plane, **Figure 1a**) generated by this equation is a feature shared by those of asymptotic equations that admit a horizontal half tangent at the asymptotic size point (Korf and Hossfeld equations). Thus, the two kinds of equations can produce similar patterns at reasonable heights. The asymptotic equations tested admit a vertical half tangent for $h = 0$. The latter can be vertical/horizontal for the SPB equation, depending on the sign of m1 m2 – 1 (Eq. 2). The fits obtained

for all tree species (**Tables 3** and **4**) for the SPB equation verified the condition m1 m2 – 1 < 0, also implying a vertical semi-tangent.

Growth equation parameterisation

Beyond the mathematical structure of equations, what parameters are allowed to vary across individuals – and what quantities they represent – also conditions their fitting accuracy. Growth equations were parameterised according to the maximal growth rate as a vertical scale parameter (R, **Figure 1a**), as it is a basically observable property (**Figure 3**). Position parameters were the height of inflection point for the SPB equation (abscissa K_R of R), and the asymptotic height (abscissa K of null growth rate, **Figure 1a**). Two parameter structures were tested: a basic one in which only parameter R varies between individual curves, and another that further includes a parameter preferentially related to late growth (asymptote K in asymptotic equations, and m2 in the SPB equation; see Eq. 5). For the SPB equation, we also tested an alternative variation in K_R. Shape parameters were assumed to be constant, to avoid overfitting of growth curves, and in line with the search for key features in species growth patterns (Richards, 1959; Zeide, 1993; **Figure 3**).

In the SPB equation, the additional between-plot variation in parameter m2 proved non-significant, in contrast to that in K_R. This suggested that the asymptotic proportionality in size curves provided by the single variation in parameter R (Eq. 5, **Figure 2**) was sufficient. However, a between-plot variation in K_R was found significant, and was found positively related to that of R in most species (**Table 3**), except for sessile oak where they were negatively correlated. A negative relationship was found for sessile oak. These results were all found consistent with those obtained from asymptotic equations: an additional variation in parameter K (**Table 3**) was found significant for all species, indicating that the convergence of top height curves towards a unique asymptote was not plausible (**Figure 3**). Also, the positive correlations found between R and K for most species (**Table 3**) suggested that the growth-related hierarchy between forest plots tended to be conserved across the ontogenetic stages covered, which is a key assumption in the concept of site index (Garcia, 2006). However, these correlations were seldom strong. In Norway spruce, the non-significant correlation was interpreted with respect to the restricted range of ages covered. Since parameters K and K_R are mathematically related in the asymptotic equations (Eq. 6), the variation in parameter K also implied a variation in K_R, and therefore correlation of the latter with R. In 3-parameter asymptotic equations, the relationship between K and K_R implies that any of these parameters can be chosen as the horizontal position parameter, as long as the shape parameter m is kept constant over a sample.

Comparison of growth equation accuracies

Regardless of the parameterisations, the SPB equation performed well. For most species, it surpassed other asymptotic equations in terms of fitting accuracy. The exceptions were observed for common beech in the one-varying-parameter scheme (better fit with Korf equation, **Table 2**), and for Corsican

pine in the two-varying-parameter scheme (better fit with Hossfeld equation, **Table 3**). The Richards equation has the fastest convergence among the equations tested and, accordingly, most often provided the worst fits. The Hossfeld equation, followed by the Korf equation, generally provided fits of intermediate quality. Residuals (**Supplementary Appendix Figure 2a**) suggested two weaknesses for the Richards equation: a growth rate increasing too slowly at low heights and an excessively fast convergence towards the asymptote (**Figure 1b**). The latter flaw was less apparent with the Hossfeld and Korf equations (**Supplementary Appendix Figures 2b** and **2c**), consistent with their slower convergence (**Figure 1b**). However, it remained strong for sessile oak, for which growth slowing was less apparent in the data (**Figure 3**), and visible but less acute in silver fir. Fits obtained with the Korf equation also provided a much more acceptable pattern at low heights (**Supplementary Appendix Figure 2c**). The explanation lies in a faster increasing expansion term in Korf (proportional to *h*, Eq. A.5) than in other equations (power <1 function of *h*, Eqs. A.3 and A.4). The residuals of the SPB equation fit over late growth exhibited a great improvement for sessile oak and were more satisfactory for silver fir and Aleppo pine (**Supplementary Appendix Figure 2d**). While statistical criteria suggested a better fit with the SPB equation for common beech in the two-varying-parameter scheme, plots of residuals remained unconvincing, and highlighted that the SPB equation was unable to reproduce the curvature observed in the data (**Figure 3**). In Corsican pine, very old stands (up to 250 yrs) were sampled and asymptotic patterns in some height curves were more salient than in other species (**Figure 3**). Interestingly, the best fit was obtained with the asymptotic Hossfeld equation (**Table 3**, **Supplementary Appendix Figures 2b** and **2d**). However, no particular flaw was identified in the SPB residuals. In general, the SPB equation fitted the observed growth patterns better than did those of the asymptotic equations at low heights. Because the power estimates for the expansion term in the SPB equation (m1 m2, Eq. 3) were very close to those of the Richards and Hossfeld equations (m), they could not account for this difference. It is thus interpreted with respect to the flexibility provided by the mathematical independence between the height of the inflection point (K_R) and the asymptotic behaviour (m2) in the SPB equation, not permitted in three-parameter asymptotic-size equations (Eq. 6). This also demonstrates the benefits of a fourth parameter in the SPB equation.

Four-parameter asymptotic sigmoid equations (with two shape parameters) have also been published (Levakovic, 1935; Garcia, 2005), but they remain largely unused. Garcia's generalisation includes most asymptotic-size growth equations as particular cases, and in particular the three equations tested in this study and the Levakovic equation. Aside from this study, we tested Garcia equation (not presented), parameterised to identify the asymptotic height (K) and the height of the inflection point (K_R) as independent position parameters, in addition to a shape parameter. Automatic fits were difficult to obtain with the *nlme* procedure, and led to manually maximising the log-likelihood (fixing/varying one shape parameter value). For parameterisation 1, the fits obtained were more accurate than those of three-parameter equations, but they remained less accurate than the SPB equation for all species (+17 to +47 AIC units) but common beech (–10 units). For parameterisation 2,

the fits obtained were found singular, as they exhibited the worst accuracy among equations tested for most species, despite other equations are nested in Garcia equation. These fits were thus set aside. While the Levakovic and Garcia equations remain important for the mathematical unification of growth equations, their expressions based on double power functions challenge the accurate statistical identification of parameters. By contrast, fits of the SPB equation revealed a systematic ease of convergence, and stability of parameter estimates with respect to initial parameter values.

The regional parameterisation was aimed at testing the ranking of growth equations when possible regional variations in shape parameters were accounted for (**Table 5**). The SPB equation remained the most accurate in all species, but the advantage of this more flexible parameterisation was not clear (**Table 5**, except in common beech where the estimate of power $1/\lambda$ was significantly smaller over one regional sample). Plots of residuals did not highlight any strong improvement for common beech, indicating an inadequacy of the SPB equation for this species.

The asymptotic-size assumption and top height growth: an ungrounded paradigm?

Prior choices in the formulation of growth equations feature the way growth patterns are analysed. When equations are based on the asymptotic assumption, the obvious indicator for describing late growth is asymptotic size. However, poor support to the asymptotic-size assumption can be found in top height growth data, even when notable ages are considered (**Figure 3**). As a consequence, asymptotic-size estimates vary widely depending on the equation fitted (**Tables 2** and **3**), which precludes any biological interpretation. The prevalent use of asymptotic-size equations in forestry therefore deserves further consideration. Whereas Knight's (1968) discussion of the issue has received significant attention, it remains marginally cited in forestry (a total 139 citations, mostly in fishery science, compared to 2 citations in forestry science; request on *scholar.google.com* dated March 7, 2012). A first explanation may lie in the implicitly higher confidence placed in asymptotic equations for extrapolation purposes. In our view, however, extrapolation is not precluded using the non-asymptotic equation proposed, since its mathematical form remains strongly constrained (sigmoid curve with decreasing late growth), and it behaved well on a growth dataset giving particular consideration to late growth. A second explanation is that asymptotic growth equations most often originated in other fields of research where asymptotic growth may be more common, including animal growth (Bertalanffy and Schnüte equations), animal and human demography (Gompertz and logistic equations), growth of plant organs (Richards equation, all cited in Zeide 1993), or crop yield (Nelder equation, Nelder, 1961). A noticeable exception is the Korf equation (Zarnovican, 1979), which interestingly exhibits a slow rate of convergence towards maximum size.

Under the non-asymptotic assumption, growth slowing over ontogeny gets quantified in terms of curvature in late-growth trajectories: the limit behaviour of height in the SPB equation was shown to allometrically scale with time (Eq. 5). The estimates for the scaling exponent $1/\lambda$ ranged from 0.20 (Corsican pine) to 0.39 (sessile oak), and from 0.26 to 0.37 when these two species were set apart

(**Table 4**). An approximation of 1/3 for this scaling coefficient would thus be reasonable for these tree species. Interestingly, this shows some similarity with Cieszewski's modification of the Hossfeld IV equation (Cieszewski, 2003): $h(t)^3 = a\, t^m / (c + t^{m-1})$, that tends toward a t (and $h(t) \rightarrow a\, t^{1/3}$ when $t >> c$).

CONCLUSIONS

Top height growth in pure and even-aged stands can be accurately described by a non-asymptotic curve, with better performances than those of asymptotic curves. The equation proposed generates sigmoid trajectories with a parabolic branch. In contrast to asymptotic-size equations, parameters related to the point of inflection and to late growth are uncorrelated. Fits were rather unconvincing for common beech, suggesting that the choice of a growth equation remains context-dependent. By contrast, fits for sessile oak emphasised that even slowly converging asymptotic equations can underestimate growth. The proposed equation admits no formal solution of time. Despite the inconvenience of numerical integration, its higher accuracy makes it worth the attention. Numerical integration methods do not require much effort to implement (**Supplementary Appendix 3**). Non-asymptotic equations should deserve more attention as soon as observational and/or theoretical bases for an upper limit to size are missing.

ACKNOLEDGEMENTS

The authors gratefully thank the French Forest Service (Office National des Forêts (ONF)) and Dr Christine Deleuze for sharing of a significant part of this dataset and for accompanying discussions. We are greatly indebted to, and thank all of those from ONF, AgroParisTech—ENGREF and INRA that participated in collecting this unique set of stem analysis data over years. We are also grateful to Prof. Oscar Garcia (University of Northern British Columbia, UNBC) for reading the manuscript and for valuable input on Garcia's (2005) growth equations. Finally, the authors wish to address their special thanks to the Associate editor, Dr Jeffrey H. Gove, and the two anonymous reviewers for providing decisive comments on improving the clarity of the manuscript and easing the presentation of the growth model.

References

Abrams, M.D., Copenheaver, C.A., Terazawa, K., Umeki, K., Takiya, M. and Akashi, N. 1999 A 370-year dendroecological history of an old-growth Abies–Acer–Quercus forest in Hokkaido, northern Japan. *Can. J. For. Res*. **29**, 1891-1899.

Bailey, R.L. and Clutter, J. L. 1974 Base-age invariant polymorphic site curves. *For. Sci*. **20**, 155-159.

Birch, C.P.D. 1999 A new generalized logistic sigmoid growth equation compared with the Richards equation. *Ann. Bot*. **83**, 713-723.

Bontemps, J.-D., Hervé, J.-C. and Dhôte, J.-F. 2009 Long-term changes in forest productivity: a consistent assessment in even-aged stands. *For. Sci*. **55**, 549-564.

Bontemps, J.-D., Hervé, J.-C. and Dhôte, J.-F. 2010 Dominant radial and height growth reveal comparable historical variations for common beech in north-eastern France. *For. Ecol. Manage*. **259**, 1455-1463.

Bontemps, J.-D., Hervé, J.-C., Leban, J.-M. and Dhôte, J.-F. 2011 Nitrogen footprint in a long-term observation of forest growth over the twentieth century. *Trees*. **25,** 237-251.

Bredenkamp, B.V. and Gregoire, T.G. 1988 A Forestry Application of Schnute's Generalized Growth Function. *For. Sci*. **34**, 790-797.

Burden, R.L. and Faires, J.D. 2001 *Numerical analysis (7th edition)*. Brooks/Cole, Pacific Grove, USA, pp. 272-282.

Cieszewski, C.J. 2003 Developing a well-behaved dynamic site equation using a modified Hossfeld IV function Y3 = axm/(c+xm-1), a simplified mixed-model and Scant subalpine fir data. *For. Sci.* **49**, 539-554.

Claessens, H., Pauwels, D., Thibaut, A. and Rondeux, J. 1999 Site index curves and autecology of ash, sycamore and cherry in Wallonia (Southern Belgium). *Forestry*. **72**, 171-182.

Curtis, R.O. 1964 A stem analysis approach to site index curves. *For. Sci*. **10**, 241-256.

Duplat, P. and Tran-Ha, M. 1997 Modélisation de la croissance en hauteur dominante du chêne sessile (Quercus petraea Liebl) en France. Variabilité inter-régionale et effet de la période récente (1959-1993). *Ann. For. Sci*. **54**, 611-634.

Ek, A. R. 1971 Size-age relationships for open-grown red pine. University of Wisconsin, *Forestry Research Notes* 156, 1-4.

Elfving, B. and Tegnhammar, L. 1996 Trends of tree growth in Swedish forests 1953-1992: an analysis based on sample trees from the National Forest Inventory. *Scand. J. For. Res*. **11**, 26-37.

Farr, W.A. and Harris, A.S. 1979 Site index of Sitka spruce along the Pacific coast related to latitude and temperatures. *For. Sci*. **25**, 145-153.

Fitzhugh, H.A. 1976 Analysis of growth curves and strategies for altering their shape. *J. Anim. Sci*. **42**, 1036-1051.

Franceschini, T., Bontemps, J.-D., Gelhaye, P., Rittié, D., Hervé, J.-C., Gégout, J.-C. and Leban, J.-M. 2010 Decreasing trend and fluctuations in the mean-ring density of Norway spruce through the twentieth century. *Ann. For. Sci*. **67**, 816.

Garcia, O. 2005 Unifying sigmoid univariate growth equations. *FBMIS*. **1**, 63-68.

Garcia, O. 2006 Site index: concepts and methods. In: *Second International Conference on Forest Measurements and Quantitative Methods and Management & The 2004 Southern Mensurationists Meeting*, Cieszewski, C.J., Strub, M., eds. Warnell School of Forestry and Natural Resources, University of Georgia, Athens, GA, USA. 275-283.

Karlsson, K. 2000 Height growth patterns of Scots pine and Norway spruce in the coastal areas of western Finland. *For. Ecol. Manage*. **135**, 205-216.

Kiviste, A. 1999 Site index change in the 1950s-1990s according to Estonian forest inventory data. In: Karjalainen, T., Spiecker, H., Laroussinie, O. (eds). Causes and consequences of accelerating tree growth in Europe. *EFI Proceedings*, EFI, Joensuu, Finland. **27**, 87-100.

Knight, W. 1968 Asymptotic growth: an example of nonsense disguised as mathematics. *J. Fish. Res. Board Can*. **25**:1303-1307.

Koch, G.W., Sillett S.C., Jennings, G.M. and Davis, S.D. 2004 The limits to tree height. *Nature*. **428**, 851-854.

Lappi, J. and Bailey, R.L. 1988 A height prediction model with random stand and tree parameters: an alternative to traditional site index methods. *For. Sci*. **34**, 907-927.

Leary, R.A. and Holdaway, M.R. 1979 Modifier function. In: A generalised forest growth projection system applied to the Lake States Region. *General Technical Report NC-49*, USDA Forest Service, USA, 31-38.

Leary, R. A., Nimerfro, K., Holdaway, M., Brand, G., Nurk, T., Kolka, R., Wolf, A. 1997 Height growth modeling using second order differential equations and the importance of initial height growth. *Forest Ecology and Management* 97, 165-172.

Lebourgeois, F., Cousseau, G. and Ducos, Y. 2004 Climate-tree-growth relationships of Quercus petraea Mill. stand in the Forest of Bercé ("Futaie des Clos", Sarthe, France). *Ann. For. Sci*. **61**, 361-372.

Levakovic, A. 1935 Analytical form of growth laws (in Serbian). *Glasnik za sumske pokuse*. **4**, 283-310.

Lindström, M.J and Bates, D.M. 1990 Nonlinear mixed effect models for repeated measures data. *Biometrics*. **46**, 673-687.

Lundqvist, B. 1957 On the height growth in cultivated stands of pine and spruce in Northern Sweden. *Medd. fran Statens Skogforsk*. **47**, 64.

Mäkelä, A. and Sievänen, R. 1992 Height growth strategies in open-grown trees. *J. Theor. Biol*. **159**, 443-467.

Minckler, L.S. 1955 Observations on open-grown, non-native conifers in southern Illinois. *Am. Mid. Nat*. **54**, 460-465.

Nelder, J. A. 1961 The fitting of a generalization of the logistic curve. *Biometrics.* **17**, 89–110.

Nord-Larsen, T., Meilby, H. and Skovsgaard, J.-P. 2009 Site-specific height growth models for six common tree species in Denmark. *Scand. J. For. Res*. **24**, 194-204.

Pienaar, L.V. and Turnbull, K.J. 1973 The Chapman-Richards generalization of Von Bertalanffy's growth model for basal area growth and yield in even-aged stands. *For. Sci*. **19**, 2-22.

Pierrat, J.-C., Houllier, F., Hervé, J.-C. and Gonzalez, R.S. 1995 Estimation de la moyenne des valeurs les plus élevées d'une population finie: application aux inventaires forestiers. *Biometrics*. **51**, 679-686.

Poage, N.J. and Tappeiner, J.C. 2002 Long-term patterns of diameter and basal area growth of old-growth Douglas-fir trees in western Oregon. *Can. J. For. Res*. **32**, 1232-1243.

Pretzsch, H. 1996 Growth trends of forests in Southern Germany. In: *Growth trends in European Forests*, Spiecker, H., Mielikäinen, K., Köhl, M., Skovsgaard, J.-P., eds. Springer, Berlin, Heidelberg, 107-131.

Richards, F.J. 1959 A flexible growth function for empirical use. *J. Exp. Bot.* **10**, 290-300.

Ryan, M.G. and Yoder, B.J. 1997 Hydraulic limits to tree height and tree growth. *BioScience*. **47**, 235-242.

Schumacher, F.X. 1939 A new growth curve and its application to timber-yield studies. *J. For.*, **37**, 819-820.

Shifley, S.R. and Brand, G.J. 1984 Chapman-Richards growth function constrained for maximum tree size. *For. Sci*. **30**, 1066-1070.

Smith, V.G. 1984 Asymptotic site-index curves, fact or artifact? *For. Chron.* **61**, 519-520.

Thomas, H. 2002 Ageing in plants. *Mech. Ageing Dev*. **123**, 747-753.

Tsoularis, A. and Wallace, J. 2002 Analysis of logistic growth models. *Math. Biosci*. **179**, 21-55.

Uhl, E., Metzger, H.-G. and Seifert, T. 2006 Dimension and growth of open-grown beech and oak trees (in German). In: *DFVVA - Sektion Ertragskunde*, Nagel J, ed., Staufen, Germany, 47-53.

Valentine, H.T. 1985 Tree-growth models: derivations employing the pipe-model theory. *J. Theor. Biol*. **117**, 579-585.

Vannière B. 1984 *Yield tables for the french forests* (2e édition). ENGREF, Nancy, France, 25 pp.

West, G.B., Brown, J.H. and Enquist, B.J. 2001 A general model for ontogenetic growth. *Nature*. **413**, 628-631.

Woodward, J. 2004 Tall storeys. *Nature*. **428**, 807-808.

Woollons, R.C., Whyte, A.G.D and Xu, L. 1990 The Hossfeld function: an alternative model for depicting stand growth and yield. *Jap. J. For.* **15**, 25-35.

Zarnovican, R. 1979 Fonction de la croissance de Korf. *For. Chron.* **55**, 194-197.

Zeide, B. 1993 Analysis of growth equations. *For. Sci*. **39**, 594-616.

Zeide, B. 2004 Intrinsic units in growth modelling. *Ecol. Mod.* **175**, 249-259.

Supplementary Appendix of:

A non-asymptotic sigmoid growth curve for top height growth in forest stands

By:

Jean-Daniel Bontemps[1,2,*], Pierre Duplat[3].

[1]AgroParisTech, ENGREF, UMR 1092 INRA/AgroParisTech Laboratoire d'Etude des Ressources Forêt-Bois (LERFoB), 14 rue Girardet, 54000 Nancy, France.

[2]INRA, Centre de Nancy, UMR 1092 INRA-AgroParisTech Laboratoire d'Etude des ressources Forêt-Bois (LERFoB), 14 rue Girardet, 54000 Nancy, France.

[3]Office National des Forêts (ONF), Département des Recherches Techniques, Boulevard de Constance, 77300, Fontainebleau, France.

* Corresponding author: jdbontemps.agroparistech@gmail.com

Supplementary Appendix 1. Late-growth behaviour of growth trajectories generated by the SPB equation

An equivalent of Eq.3 for high values of *h* is given by:

$$dh/dt \sim R / m1 \, (h/K_R)^{\,m2(m1-1)} \qquad \text{when} \quad h >> 1 \qquad (A.1)$$

Integration of Eq. A.1 (see Appendix 2 for integration) leads to an explicit limit solution:

$$h(t) \sim (R \, \lambda \, K_R^{\,\lambda - 1} / m1)^{\,1/\lambda} \, t^{\,1/\lambda} \quad \text{when} \quad t >> 1 \qquad (A.2)$$

where: $\lambda = 1 + m2 \, (1 - m1)$.

An example of the SPB trajectory (numerical integration of the SPB equation, see Supplementary Appendix 3) is provided in Figure 1 below. The explicit limit solution (with the same parameter values) is superimposed onto this trajectory, with different age-height initial conditions.

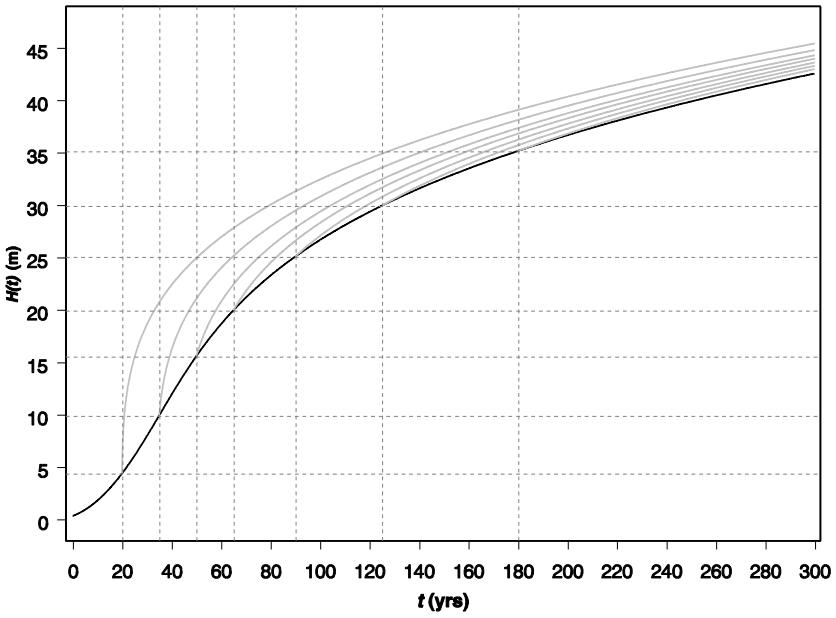

Supplementary Appendix Figure 1. Trajectory generated by the SPB equation (Eq. 3, black line) and approximations of the late growth trajectory (grey lines) based on the explicit limit solution to this equation (Eq. 5). Parameter values for the SPB trajectory are given by {R = 0.4 m.yr^{-1}, K_R = 10 m, m1 = 0.15, m2 = 3.2}. The explicit limit solution is plotted for different initial conditions of age-height pairs, defined from regularly (~5 m) spaced heights ranging from 5 to 35 m, positioned at round ages: {20 yrs, 4.36 m}, {35 yrs, 9.89 m}, {50 yrs, 15.54 m}, {65 yrs, 19.93 m}, {90 yrs, 25.05 m}, {125 yrs, 29.91 m}, and {180 yrs, 35.13 m}.

The explicit limit solution well illustrates the horizontal parabolic branch of the trajectory generated by the SPB equation over late-growth. While the successive approximations defined by this limit

solution get closer to the exact trajectory, they are of course not sigmoid (see Eqs. 4 and 5) and are not intended to define a substitute to the SPB equation.

Supplementary Appendix 2. Growth equations of the asymptotic sigmoid growth curves tested

1. First-order differential equations

R ($m.yr^{-1}$) is the maximal growth rate, K (m) is the asymptotic size, m (dimensionless) is the shape parameter and K_R (m) is the height of the inflection point.

Richards equation

$$\frac{dh}{dt} = \mathrm{R}\ \mathrm{C_m}\ \left(\frac{h}{\mathrm{K}}\right)^{1-\mathrm{m}} \left(1-\left(\frac{h}{\mathrm{K}}\right)^{\mathrm{m}}\right) \qquad \text{(A.3)}$$

With: $\mathrm{C_m} = (1-\mathrm{m})^{(\mathrm{m}-1)/\mathrm{m}} / \mathrm{m}$ and $\mathrm{m} < 1$

Height of the inflection point: $\mathrm{K_R} = \mathrm{K}\left(1-\mathrm{m}\right)^{1/\mathrm{m}}$

Hossfeld equation

$$\frac{dh}{dt} = \mathrm{R}\ \mathrm{C_m} \left(\frac{h}{\mathrm{K}}\right)^{1-\mathrm{m}} \left(1-\frac{h}{\mathrm{K}}\right)^{1+\mathrm{m}} \qquad \text{(A.4)}$$

With: $\mathrm{C_m} = 4\,(1-\mathrm{m})^{(\mathrm{m}-1)}\,(1+\mathrm{m})^{-(1+\mathrm{m})}$ and $\mathrm{m} < 1$

Height of the inflection point: $\mathrm{K_R} = \dfrac{\mathrm{K}\left(1-\mathrm{m}\right)}{2}$

Korf equation

$$\frac{dh}{dt} = \mathrm{R}\ \mathrm{C_m} \left(\frac{h}{\mathrm{K}}\right)\left(ln\left(\frac{\mathrm{K}}{h}\right)\right)^{1+\mathrm{m}} \qquad \text{(A.5)}$$

With: $\mathrm{C_m} = exp\left(\left(1+\mathrm{m}\right)\left(1-ln\left(1+\mathrm{m}\right)\right)\right)$

Height of the inflection point: $\mathrm{K_R} = \dfrac{\mathrm{K}}{exp\left(1+\mathrm{m}\right)}$

2. Analytical solutions

Each growth equation as the general following expression:

$$\frac{dh}{dt} = R\,C_m\ f\left(h\right)$$

Leading to the following differential form:

$$\frac{dh}{f(h)} = \mathrm{R\ C_m}\ dt$$

By calculating $F_1(u) = \int \frac{du}{f(u)}$ and $F_2(v) = \int dv$, and computing these integrals on a time interval $[t_0, t]$, we obtain:

$$F_1(h(t)) - F_1(h(t_0)) \quad = \quad \mathrm{R\ C_m}\ (t - t_0)$$

Finally:

$$F_1(h(t)) \quad = \quad F_1^{-1}(\mathrm{R\ C_m}\ (t - t_0) + F_1(h(t_0)))$$

This procedure was applied to obtain the following analytical solutions.

Richards equation

$$h(t) \ = \ \mathrm{K}\left[1 \ + \ \left(\left(\frac{h(t_0)}{\mathrm{K}}\right)^{\mathrm{m}} - 1\right) exp\left(-\frac{\mathrm{R\,m\,C_m}}{\mathrm{K}}(t - t_0)\right)\right]^{\frac{1}{\mathrm{m}}} \qquad \text{(A.6)}$$

Hossfeld equation

$$h(t) \ = \ \frac{\mathrm{K}}{1 + \left[\frac{\mathrm{R\,m\,C_m}}{\mathrm{K}}(t - t_0) + \left(\frac{h(t_0)}{\mathrm{K} - h(t_0)}\right)^{\mathrm{m}}\right]^{-\frac{1}{\mathrm{m}}}} \qquad \text{(A.7)}$$

Korf equation

$$h(t) \ = \ \mathrm{K}\ exp\left[-\left(\frac{\mathrm{R\,m\,C_m}}{\mathrm{K}}(t - t_0) \ + \left(ln\frac{\mathrm{K}}{h(t_0)}\right)^{-\mathrm{m}}\right)^{-\frac{1}{\mathrm{m}}}\right] \qquad \text{(A.8)}$$

3. Limit approximations to these analytical solutions (late growth behaviour)

These equivalents were calculated based on the fundamental equivalents, and by considering that the initial condition $h(t_0)$ is small relative to K.

An equivalent for the Richards equation is:

$$h(t) \approx \mathrm{K}\left(1-\left(\frac{1}{\mathrm{m}\ exp\left(\mathrm{C}\,t\right)}\right)\right) \qquad \text{for } t >> 1 \qquad \text{(A.9)}$$

Equivalents for the Korf and Hossfeld equations are given by:

$$h(t) \approx \mathrm{K}\left(1-\frac{1}{\left(\mathrm{C}\,t\right)^{1/\mathrm{m}}}\right) \qquad \text{for } t >> 1 \qquad \text{(A.10)}$$

With: $C = R\ m\ C_m / K$ in both cases.

Supplementary Appendix 3. Runge-Kutta 4 numerical integration algorithm for a first order autonomous differential equation, and use in combination with the *nlme* function (non-linear mixed-effect models) in R/S code

The SPB equation has no analytical solution of time, and must be numerically integrated. The SPB equation was fitted onto non-overlapping forward difference data, using the *nlme* function (non-linear mixed-effects models). Therefore, it was required to develop a function, called by *nlme* performing the numerical integration on any height increment of the dataset. We used the Runge-Kutta 4 numerical integration method (Burden and Faires 2001, pp 272-282).

We present the R/S code to define functions computing: (1) the 4th-order Runge-Kutta numerical integration of an autonomous first-order differential equation (function **Integration.RK4**), (2) the particular SPB equation (function **SPB**, called by **Integration.RK4**). We further give an example of call of **nlme**, combining Integration.RK4 and SPB. The parameterisation corresponds to a fit of the SPB equation with parameterisation 2 (Table 3).

1. Function "Integration.RK4 ( )"

```
Integration.RK4 <- function (p, x0, dt, n, GrowthEq = SPB)

{

  # This function computes the numerical integration (4th-order Runge-Kutta integration method) of an
  autonomous differential equation of order 1, whose expression is defined by the function "SPB".

  # growthEq is a growth function, defined by default as the "SPB" function
  # p is the parameter vector of the growth equation
  # x0 is the initial condition of the state variable (here initial height) defined by the differential equation
  # dt is the time interval on which to compute the numerical integration
  # n is the number of steps (subintervals of dt) used to compute numerical integration.

  step <- dt/n
```

```
  for(i in 0:(n - 1))
  {
    if(i == 0) xEnd <- x else xEnd <- xNext

    k1 <- growthEq (p, xEnd)
    k2 <- growthEq (p, xEnd + step/2 * k1)
    k3 <- growthEq (p, xEnd + step/2 * k2)
    k4 <- growthEq (p, xEnd + step * k3)
    xNext <- xEnd + step/6 * (k1 + 2 * k2 + 2 * k3 + k4)
  }

  xNext
}
```

2. Function "SPB"

```
SPB <- function (p, x)

{

  # This function computes the absolute growth rate of the SPB equation, for a state "x" of the state
  variable (here height) and the parameter vector p.

  # note : p = c(R, KR, m1, m2) (see Eq. 5) of the manuscript.

  (p[1] * (x/p[2])^(p[3] * p[4]))/(1 - p[3] + p[3] * (x/p[2])^p[4])

}
```

3. Call to "nlme"

In this example, the dataset "Oak" is organised as non-overlapping forward difference data. Thus, it includes the variables: 1) "H" and "Hstart", corresponding to the initial and final heights of any increment, 2) the variable "dt", the duration of the height increment, and 3) the variable "Plot", a factor to gather the height data according to their plot origin, used for random effects. In this parameterisation of the SPB model, parameters R and m2 include a random effect at the "plot" level. The model is named "Oak.SPB.Rm2.nlme". The number of integration steps for any height increment is 25. The following expression is typed in the "Command Window" of R/S-PLUS:

```
> Oak.SPB.Rm2.nlme <- nlme (model = H ~ Integration.RK4 (c(R, KR, m1, m2), Hstart, dt, 25,
"SPB"), data = Oak, fixed = list(R + KR + m1 + m2 ~ 1), random = list (Plot = R + m2 ~ 1), start =
c(0.4, 7, 0.1, 2), verbose = T)
```

Note: an R package (http://www.r-project.org) to include numerical integration in a call to *nlme*, named *nlmeODE*, has recently been released on R (January 14. 2010). It uses the second package DEsolve (released on August 10. 2011). These packages were not used in the present study, as these were not available when the authors designed the **Integration.RK4** and **SPB** code. They provide extended solutions for numerical integration, including different methods (of which the Euler, RK2 and RK4 methods, and methods with an adaptive time step), for different initial value problems (systems of equations, non autonomous equations, ...). While we did evaluate this package in-depth,

we draw attention onto the fact that, while the present code is surely restricted with respect to the variety of situations where numerical integration is needed, it however remains of a very straight access.

Supplementary Appendix 4. Analyses of model residuals

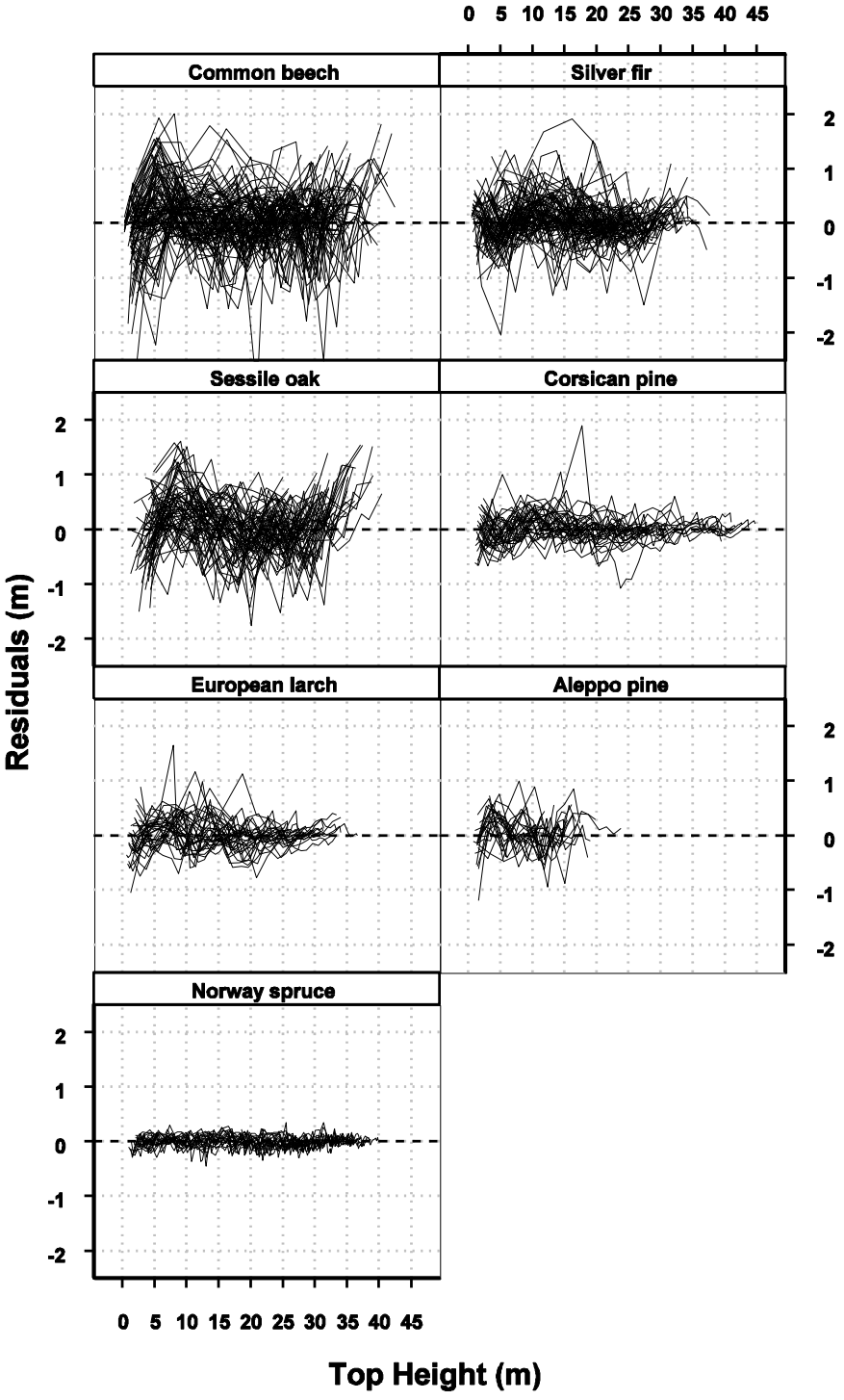

Supplementary Appendix Figure 2a. Model residuals against height for the Richards equation fits. The fits were performed with parameterisation 2 (Table 3).

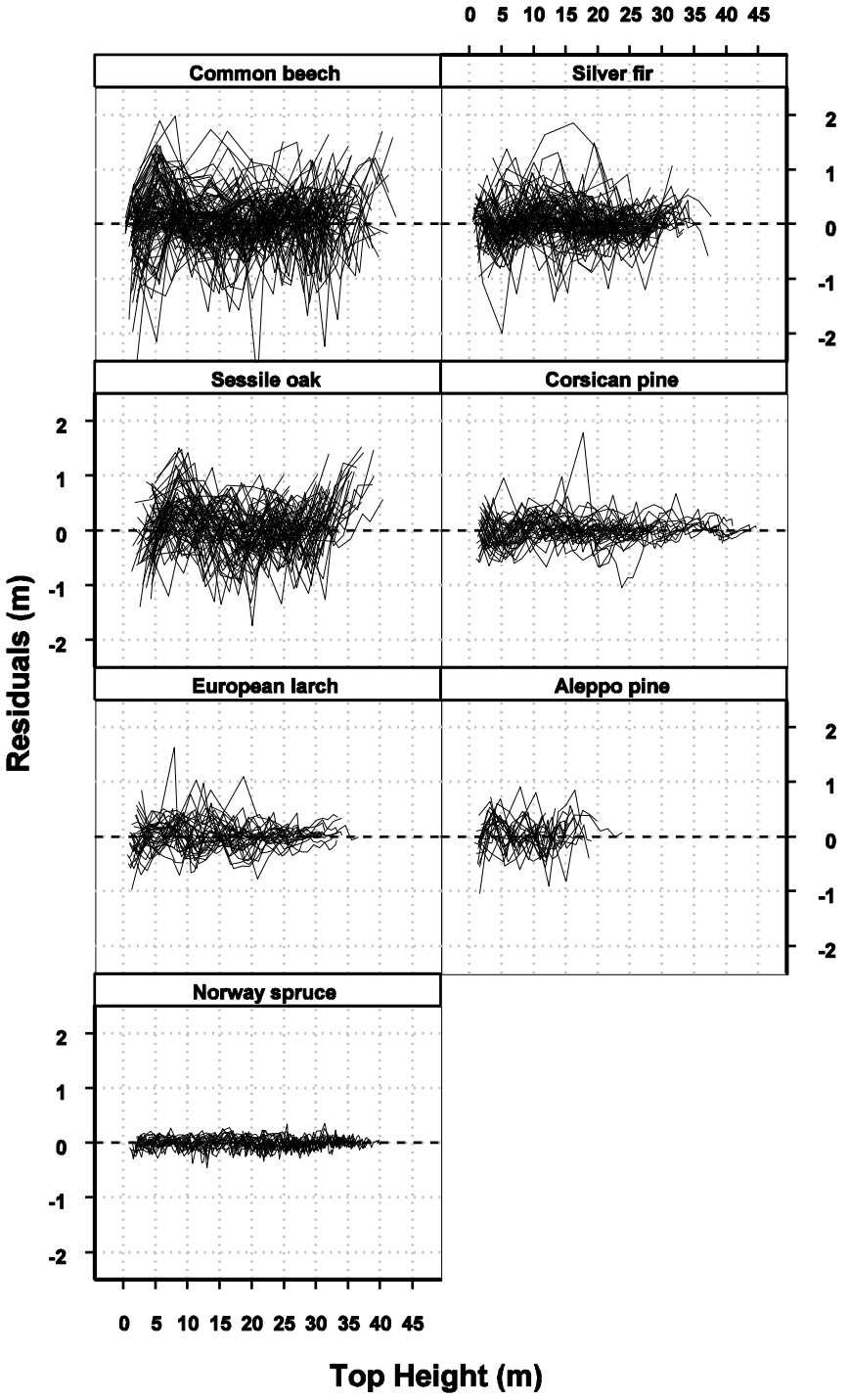

Supplementary Appendix Figure 2b. Model residuals against height for the Hossfeld equation fits. The fits were performed with parameterisation 2 (Table 3).

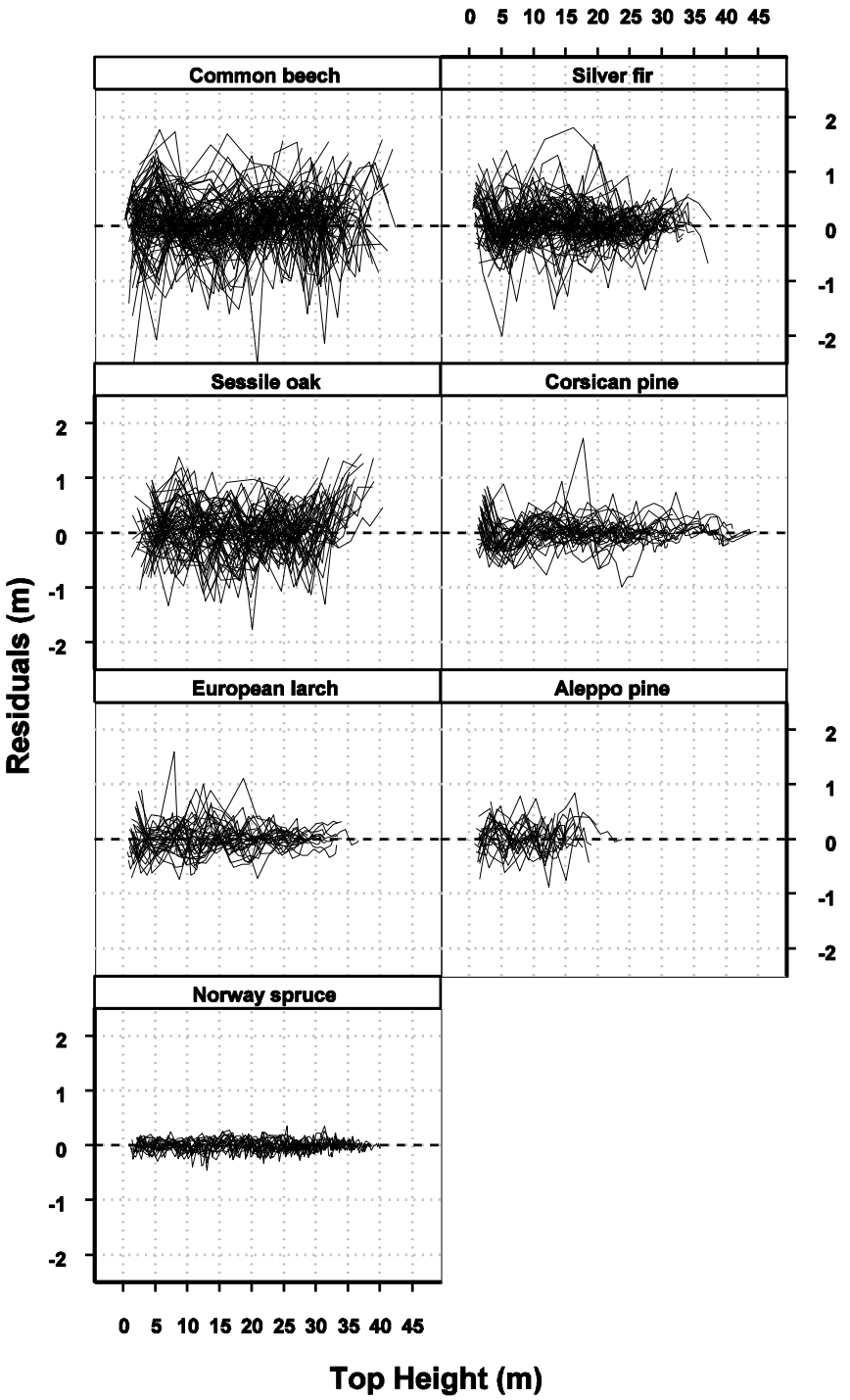

Supplementary Appendix Figure 2c. Model residuals against height for the Korf equation fits. The fits were performed with parameterisation 2 (Table 3).

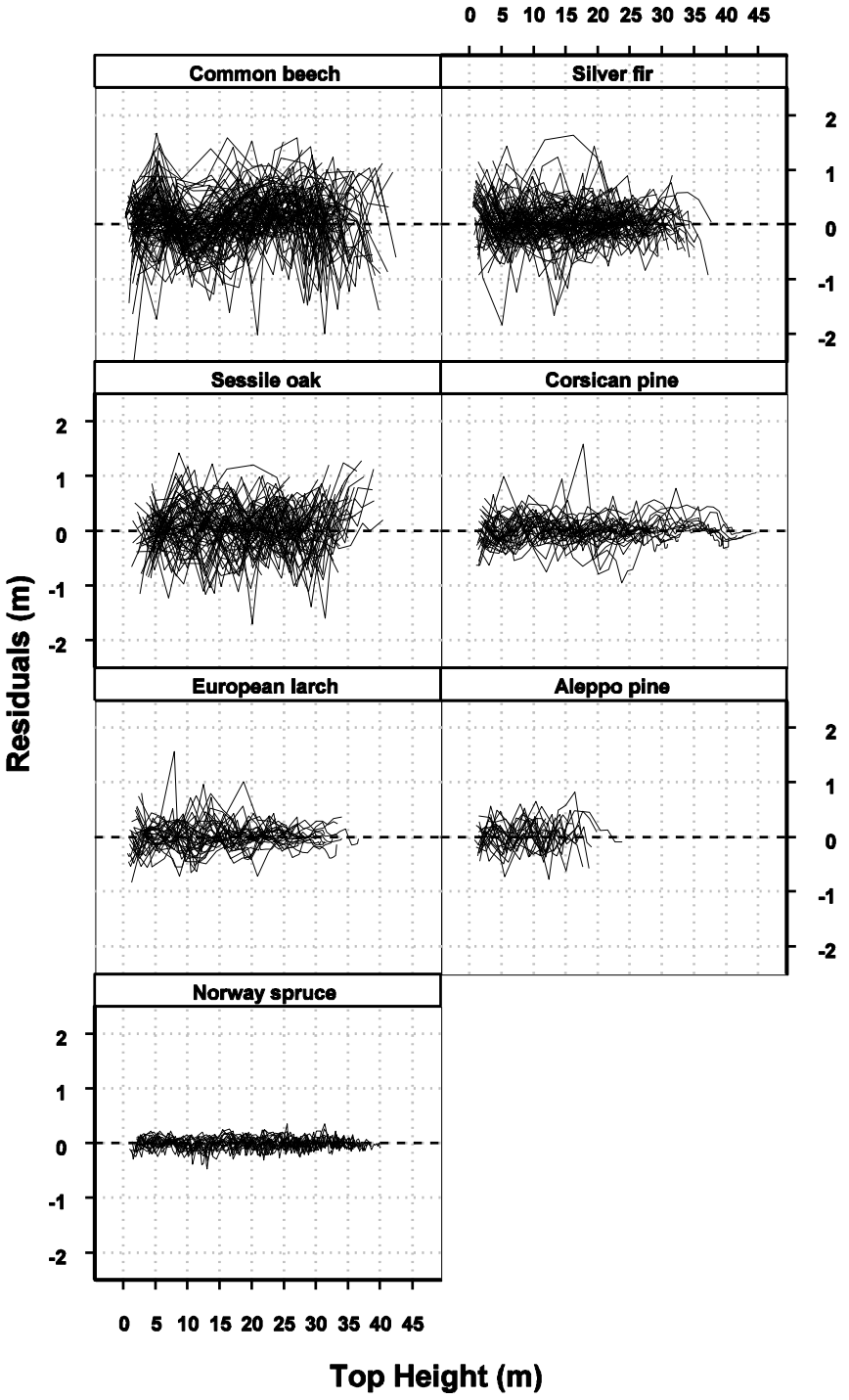

Supplementary Appendix Figure 2d. Model residuals against height for the SPB equation fits. The fits were performed with parameterisation 2 (Table 3).

Analysis of model residuals for parameterisation 2.

Fits obtained with the Richards equation (Figure 2a) revealed systematic underestimation for heights between 5 and 10 m and at the extremity of height curves. These biases were less obvious for Corsican pine and European larch. The same biases were observed with the Hossfeld equation (Figure 2b), with a slightly lower magnitude for European larch and Corsican pine. Underestimation at low heights was reduced using the Korf equation (Figure 2c) for common beech, sessile oak, European larch and Aleppo pine. By contrast, initial growth (0-5 m) was underestimated for silver fir, Corsican pine, and European larch. For most species, underestimation of late growth was also reduced with the Korf equation. Residuals in sessile oak suggested that even the Korf equation underestimated late growth (Figures 1b and 3). A slight height overestimation could be detected in Corsican pine, for which asymptotic patterns were detected (Figure 3). Residual plots obtained with the SPB equation revealed no apparent bias across the range of tree height for all species but for common beech (Figure 2d). Abnormal curvatures in residuals of initial growth were no longer apparent in silver fir and Corsican pine. Late growth was also more correctly estimated for sessile oak and silver fir. Overestimation for late growth in Corsican pine remained. In common beech, residuals obtained with the SPB equation showed height overestimation at around 10 m and at late growth, and underestimation between 20 and 30 m. This suggested that the equation was unable to predict the rather strong concavity of height curves in that area as compared with other species (Figure 3).

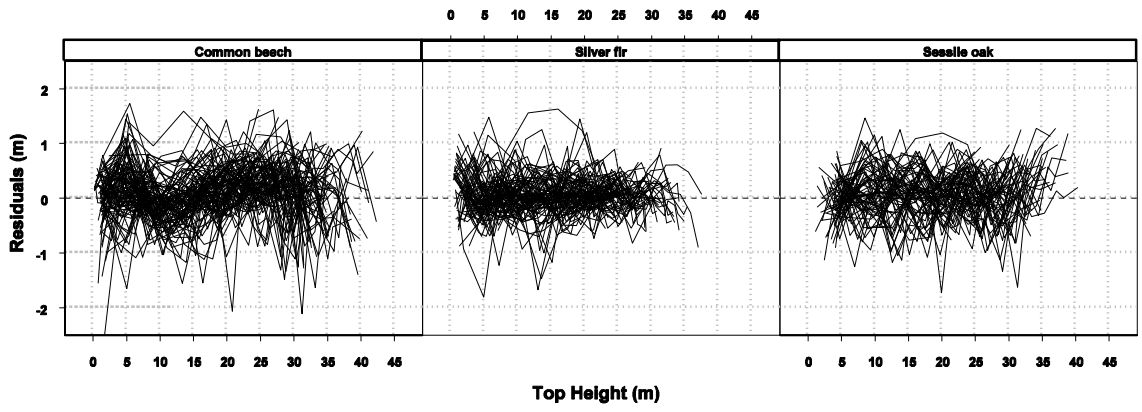

Supplementary Appendix Figure 3. Model residuals against height for the SPB equation fits allowing regional parameterisation (parameterisation 3) in the shape parameter (see Tables 1 and 5).

Supplementary Appendix Figure 4. Comparison of trajectories fitted with the Hossfeld IV, Korf and SPB growth models. Models were fitted with parameterization 2. For each species, one plot was selected from Figure 4 to cover a maximum age range. Dark grey: empirical top height growth curve, pink: Hossfeld IV equation, blue: Korf equation, green: SPB equation.

1. Common Beech

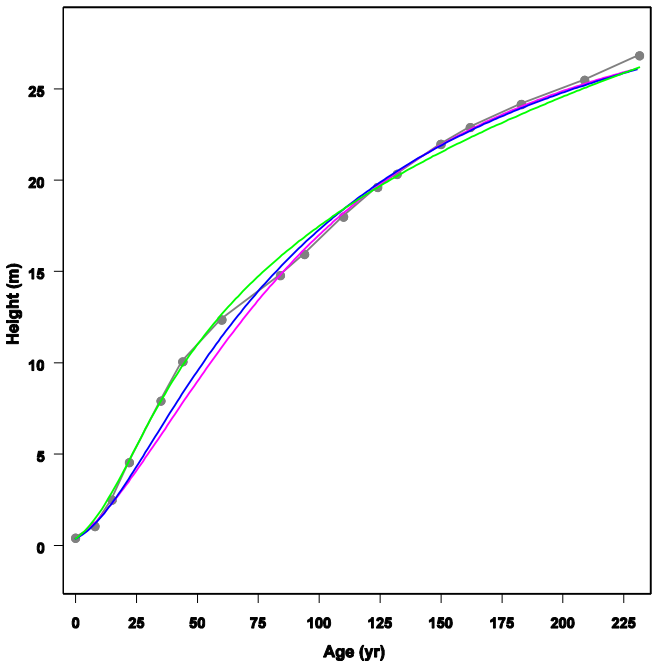

2. Silver Fir

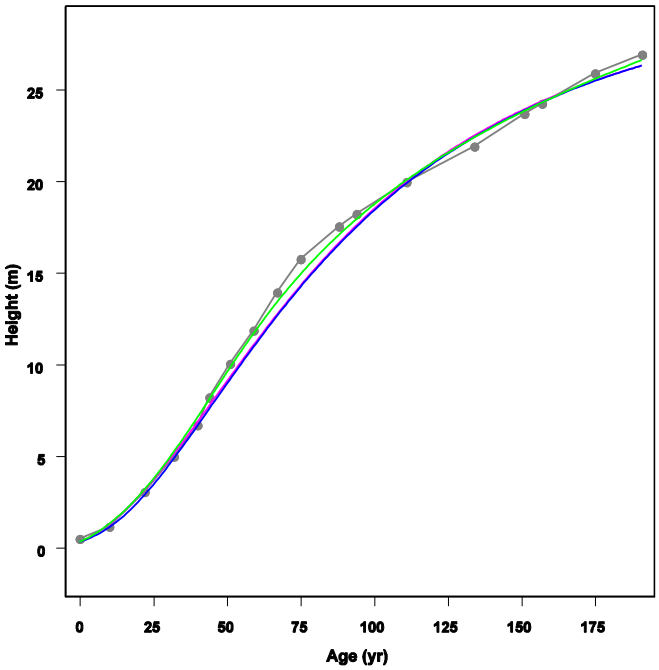

3. Sessile oak

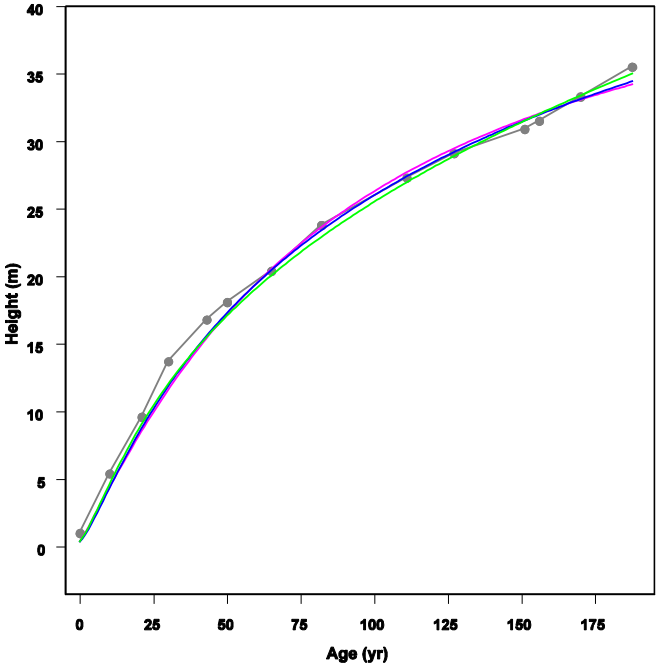

4. Corsican pine

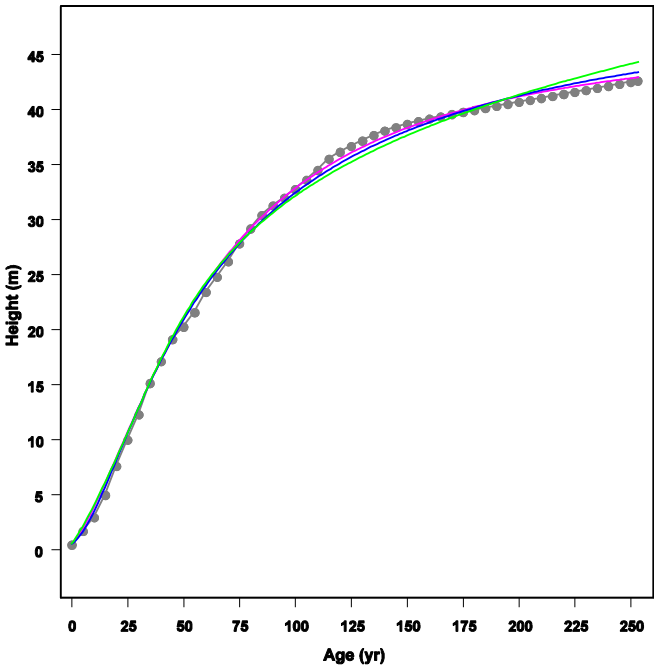

5. European larch

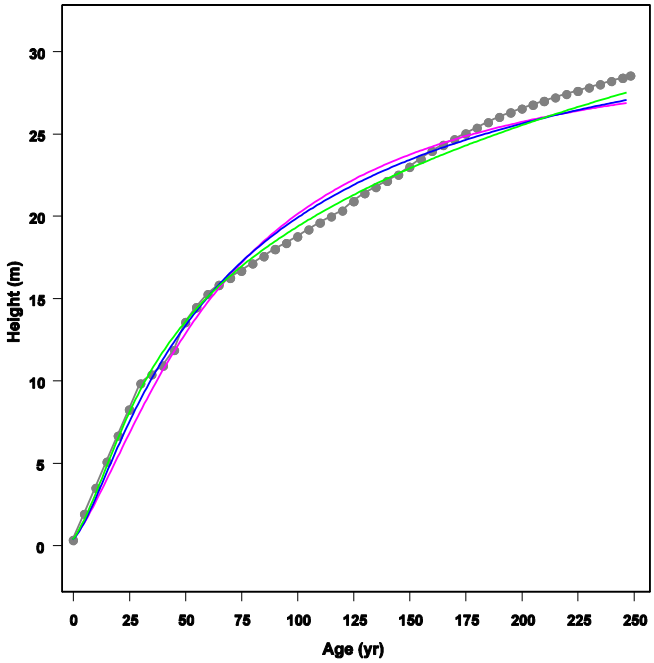

6. Aleppo pine

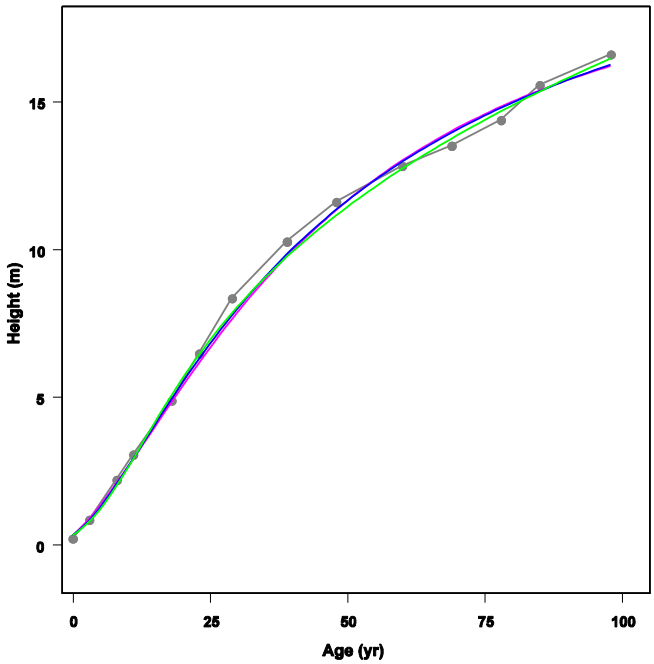

7. Norway spruce